

**NOAA**  
**FISHERIES**

Alaska Fisheries Science Center  
Resource Assessment and Conservation Engineering Division  
Midwater Assessment and Conservation Engineering Program

# Results of the February 2020 Acoustic-Trawl Survey of Walleye Pollock (*Gadus chalcogrammus*) Conducted in the Southeastern Aleutian Basin near Bogoslof Island, Cruise DY2020-02

SEPTEMBER 2023

## AFSC Processed Report

This document should be cited as follows:

McKelvey, D., and Levine, M. 2023. Results of the February 2020 acoustic-trawl survey of walleye pollock (*Gadus chalcogrammus*) conducted in the southeastern Aleutian Basin near Bogoslof Island, Cruise DY2020-02. AFSC Processed Rep. 2023-04, 67 p. Alaska Fish. Sci. Cent., NOAA, Natl. Mar. Fish. Serv., 7600 Sand Point Way NE, Seattle WA 98115.

This document is available online at: <https://repository.library.noaa.gov/>

Reference in this document to trade names does not imply endorsement by the National Marine Fisheries Service, NOAA.

**Results of the February 2020 Acoustic-Trawl Survey  
of Walleye Pollock (*Gadus chalcogrammus*)  
Conducted in the Southeastern Aleutian Basin  
Near Bogoslof Island, Cruise DY2020-02**

by Denise McKelvey and Mike Levine

Resource Assessment and Conservation Engineering Division  
Alaska Fisheries Science Center  
NOAA, National Marine Fisheries Service  
7600 Sand Point Way NE  
Seattle, WA 98115

September 2023

THIS INFORMATION IS DISTRIBUTED SOLELY FOR THE PURPOSE OF PRE-DISSEMINATION PEER REVIEW UNDER APPLICABLE INFORMATION QUALITY GUIDELINES. IT HAS NOT BEEN FORMALLY DISSEMINATED BY NOAA FISHERIES/ALASKA FISHERIES SCIENCE CENTER AND SHOULD NOT BE CONSTRUED TO REPRESENT ANY AGENCY DETERMINATION OR POLICY



## CONTENTS

ABSTRACT.....	v
INTRODUCTION .....	1
METHODS .....	1
Acoustic Equipment, Calibration, and Data Collection.....	2
Trawl Gear and Oceanographic Equipment.....	3
Survey Design.....	5
Data Analysis .....	7
Processing acoustic data .....	7
From backscatter to abundance, an overview .....	7
Selectivity correction .....	7
Male-female ratio adjustment (equal-sex correction).....	8
Abundance calculations .....	9
Maturity data processing.....	10
Pollock vertical distribution.....	11
Relative estimation error.....	12
Sensitivity analysis.....	13
RESULTS AND DISCUSSION .....	14
Survey Weather Detours .....	14
Calibration.....	14
Survey Coverage.....	15
Water Temperature .....	15
Trawl Samples .....	15
Distribution and Abundance .....	17
Sensitivity Analysis .....	18
Survey Time Series and Future Directions .....	19
ACKNOWLEDGMENTS .....	21
CITATIONS .....	23

TABLES .....	28
FIGURES .....	43
APPENDICES .....	59

## ABSTRACT

Scientists from the Alaska Fisheries Science Center conducted an acoustic-trawl (AT) survey in mid-February 2020 to estimate the abundance of pre-spawning walleye pollock (*Gadus chalcogrammus*) in the southeastern Aleutian Basin near Bogoslof Island. Twenty-six transect lines were surveyed, and 14 trawl hauls were conducted for biological measurements during the survey. This report summarizes the observed pollock distribution and biological information and provides an abundance estimate used for stock assessment.

The 2020 Bogoslof AT survey measured pollock across the entire region surveyed. Most of the pollock (88%) was distributed in the Samalga region. Pollock dominated the trawl catches and ranged 29-69 cm in length with a mode at about 53 cm fork length. The estimated numbers of pollock in 2020 were 338 million fish with a biomass of 353 thousand metric tons (t). This was a 47% decrease in biomass from the 2018 estimate (663 thousand t). Seventy-seven percent of the estimated 2020 biomass were 9- to 11-year-old fish from the 2011-2009 year classes.

Improvements in the gear and analysis method marks the 2020 abundance and biomass estimates. This was the first survey in the Bogoslof time series that the LFS1421 net was used as the primary sampling tool. Additionally, this was the first survey in the time series that allocated backscatter to all species based on catch from the nearest-trawl haul. Other improvements include an abundance-weighted maturity composition, and net-selectivity corrections. Lastly, due to the calculations for the above analysis improvements, the equal-sex correction was not applied so the long-held assumption that the pollock population in the Bogoslof region has a 50:50 sex ratio was dropped from the primary analysis. When sensitivity of results to those changes was examined, and differences of 1-3% in biomass and 1-7% in abundance were indicated.





## INTRODUCTION

Scientists from the Midwater Assessment and Conservation Engineering (MACE) Program of the Alaska Fisheries Science Center (AFSC) regularly conduct acoustic-trawl (AT) surveys in late February and early March to estimate the abundance of pre-spawning walleye pollock (*Gadus chalcogrammus*; hereafter referred to as “pollock”) in the southeastern Aleutian Basin near Bogoslof Island (Honkalehto et al. 2008). These surveys were conducted annually between 1988 and 2007 (with the exception of 1990 and 2004), and biennially starting in 2009 (with the exception of 2011). The biomass estimate for pollock within the Central Bering Sea (CBS) Convention Specific Area obtained during these AT surveys provides an index of abundance representing 60% of the Aleutian Basin pollock stock<sup>1</sup>. Therefore, when the pollock biomass estimate from this survey surpasses 1 million metric tons (t), the Aleutian Basin pollock stock surpasses a 1.67 million t threshold above which targeted pollock fishing in the Aleutian Basin can be negotiated. This report summarizes observed pollock distribution and biological information from the winter 2020 AT survey, provides an abundance estimate used for stock assessment (Ianelli et al. 2020), and summarizes water temperature observations and acoustic system calibration results.

## METHODS

An acoustic-trawl survey of walleye pollock in the southeastern Aleutian Basin near Bogoslof Island was conducted by MACE scientists between 19 and 23 February 2020, which was 2 weeks earlier in 2020 than the survey in the winter 2018. The survey was conducted aboard the NOAA ship *Oscar Dyson* (cruise DY2020-02), which is a 64-m stern trawler equipped for fisheries and oceanographic research. Although the primary goal was to assess the abundance and distribution of pre-spawning pollock in the Bogoslof Island area between about 167°W (Unalaska Island) and 170°W (Islands of Four Mountains), supplemental trawl sampling was

---

<sup>1</sup> Convention on the Conservation and Management of Pollock Resources in the Central Bering Sea, Annex (Part 1), Treaty Doc. 103-27. 1994. Hearing before the Committee on Foreign Relations U.S. Senate, 103<sup>rd</sup> Congress, 2<sup>nd</sup> Session. Washington: U.S. Government Printing Office.

also conducted in the Shumagin Islands for the prior cruise DY2020-01, and in Shelikof Strait for the subsequent cruise DY2020-03. Surveys followed established AT methods as specified in NOAA protocols for fisheries acoustics surveys and related sampling<sup>2</sup>. The acoustic units used here are defined in MacLennan et al. (2002). Survey itineraries are listed in Appendix I and scientific personnel in Appendix II.

### Acoustic Equipment, Calibration, and Data Collection

Acoustic measurements were collected with Simrad EK80 scientific echosounding system (Demer et al. 2017). The Simrad EK80 transceiver pinged nominally once every 1-2 seconds triggering six split-beam transducers (18-, 38-, 70-, 120-, 200-, 333-kHz) mounted on the bottom of the vessel's retractable centerboard. The centerboard was extended to a depth of 9.15 m during the survey. System electronics were housed inside the vessel in a permanent laboratory space dedicated to acoustics.

Two standard sphere acoustic system calibrations were conducted in Alaska to measure acoustic system performance (Table 1). The vessel's dynamic positioning system was used to maintain the vessel location during calibrations. Local water temperature and salinity were measured and used to estimate absorption and sound speed. A tungsten carbide sphere (38.1 mm diameter) suspended below the centerboard-mounted transducers was used to calibrate the 38-, 70-, 120-, and 200-kHz systems. The tungsten carbide sphere was then replaced with a 64 mm diameter copper sphere to calibrate the 18-kHz system. The 333-kHz frequency was not calibrated due to unexplained noise that obscured the majority of the water column on the 333 kHz frequency. A two-stage calibration approach was followed for each frequency calibrated. On-axis sensitivity (i.e., transducer gain and Sa correction) was estimated from measurements with the sphere placed in the center of the beam following the procedure described in Foote et al. (1987). Transducer beam characteristics (i.e., beam angles and angle offsets) were estimated by moving the sphere in a horizontal plane using the EK80's calibration utility (Simrad, 2018, Jech et al.

---

<sup>2</sup>National Marine Fisheries Service (NMFS) 2014. NOAA protocols for fisheries acoustics surveys and related sampling (Alaska Fisheries Science Center), 26 p. Prepared by Midwater Assessment and Conservation Engineering Program, Alaska Fish. Sci. Center, Natl. Mar. Fish. Serv., NOAA. Available upon request.

2005). The equivalent beam angle (used to characterize the volume sampled by the beam) and angle sensitivities (for conversion of electrical to mechanical angles) cannot be estimated using this calibration approach because the absolute position of the sphere was unknown (Demer et al. 2017). Thus, the transducer-specific equivalent beam angle and angle sensitivities measured by the echosounder manufacturer were used during calibration.

Acoustic data were collected between 16 m from the ocean surface to 1,000 m depth, 24 hours/day, and bottom depths were measured to 1,500 m depth. Raw acoustic data from the six frequencies were logged using EK80 software (v. 1.12.4), and EchoLog 80 (v. 8.0.4.0) broadcasted raw files. The average sounder-detected bottom line was calculated using 3 to 5 frequencies, depending on the depth (Jones et al. 2011).

Data were analyzed using Echoview post-processing software (v. 10.0.298). Fish abundance and distribution results presented here are based on 38 kHz acoustic backscatter integrated using a post-processing  $S_v$  integration threshold of -70 decibels (dB re  $1 \text{ m}^{-1}$ ).

#### Trawl Gear and Oceanographic Equipment

Midwater and near-bottom acoustic backscatter was sampled using an LFS1421 and an Aleutian Wing 30/26 Trawl (AWT). The headrope and footrope of the LFS1421 each measure 76.8 m (252 ft), with meshes tapering from 650 cm (256 in) in the forward sections to 3.8 cm (1.5 in) in the section immediately preceding the codend. The codend was made of 8.9 cm (3.5 in) mesh and was fitted with a codend liner composed of knotless nylon 7.9 mm (5/16 in) stretched mesh (3.2 mm (1/8 in) square opening) to increase retention of small organisms. The AWT headrope and footrope each measure 81.7 m (268 ft) and mesh sizes taper from 325.1 cm (128 in) in the forward section of the net to 8.9 cm (3.5 in) in the codend, which was fitted with a 12.7 mm (1/2 in) codend liner.

This is the first survey in the Bogoslof region where the LFS1421 replaced the AWT as the primary sampling trawl. The species composition and size distribution in the catches of the two nets were compared to determine if the nets had any significant differences in catch. Given that

the LFS1421 net's codend liner is 3.2 mm, and the AWT's codend liner is 12.7 mm, we expected more retention of smaller organisms in the LFS1421 net than the AWT. To facilitate this comparison, time was devoted to paired trawling, at the same location and depth, whenever possible during the survey.

The LFS1421 was fished with four 45.7 m (150 ft) bridles and the AWT was fished with four 82.3 m (270 ft) bridles (1.9 cm (0.75 in) dia.). Both were fished with two 5 m<sup>2</sup> Fishbuster trawl doors (1,247 kg (2,750 lb) each). The LFS1421 was fished either with 227 kg (500 lb), 340 kg (750 lb), or 454 kg (1000 lb) tom weights attached to each wingtip, while the AWT was fished either with 227 kg (500 lb) or 340 kg (750 lb) tom weights. Average trawling speed was approximately 1.75 m/sec (3.4 knots) for the LFS1421 and 1.7 m/sec (3.3 knots) AWT. Vertical net openings and headrope depths were monitored with a Simrad FS70, third-wire netsonde attached to the headrope. The vertical net opening of the LFS1421 ranged from 6.5 to 26.8 m and averaged 17.1 m while fishing. The vertical mouth opening of the AWT ranged from 21.5 to 36 m and averaged 29.9 m while fishing.

Recapture (or pocket) nets were placed at several locations along the LFS1421 net (Williams et al. 2011) and the AWT net. The LFS1421 trawl was fitted with 9 nine recapture nets placed on the forward (813 mm stretch mesh), mid (102 mm stretch mesh), and aft (102 mm stretch mesh) sections of the trawl, one recapture net on the top, bottom, and port panel of each section. The recapture nets were constructed from 3.2 mm (1/8 inch) mesh. Recapture nets were not attached to the AWT trawl samples conducted in the Bogoslof area but they were attached to the trawl for the Shelikof Strait trawl sample. Before the Shelikof AWT deployment, the AWT was fitted with a total of eight recapture nets constructed from heavy delta nylon 12.7 mm (1/2 in) stretched mesh (matching the codend liner), with one placed on the top, bottom, port, and starboard panels of the mid (406 mm stretch mesh) and aft (102 mm stretch mesh) sections of the net. Catch in the recapture nets was recorded independently from the catch in the codend. These data are being used in ongoing work to estimate the trawl selectivity of the midwater nets and to gauge escapement of juvenile pollock and other small fishes (see Appendix III).

A stereo camera system (CamTrawl; Williams et al. 2010) was also attached to the starboard panel forward of the codend on both the LFS1421 and AWT nets. The CamTrawl was used to capture stereo images for species identification and length measurement of individual fish as they pass through the net toward the codend. The CamTrawl data are useful in determining size and species composition of fish when distinct and separate backscatter layers are sampled by a trawl haul but could not be differentiated in the trawl catch. Images were viewed and annotated using procedures described in Williams et al. (2010).

Physical oceanographic measurements were collected throughout the cruise. Temperature-depth profiles were obtained at trawl sites with a Sea-Bird Electronics temperature-depth probe (SBE-39) attached to the trawl headrope. Sea surface temperature data were measured using the ship's calibrated Sea-Bird Electronics sea surface temperature system (SBE 38, accuracy  $\pm 0.002^{\circ}\text{C}$ ). If the SBE 38 was not operating, sea surface temperatures were taken from the mid-ship Furuno T-2000 temperature probe (accuracy  $\pm 0.2^{\circ}\text{C}$ ) located 1.4 m below the surface. During this survey, the SBE 38 was used 94.4% of the time. Surface temperatures were averaged to 0.5 nautical mile (nmi) intervals for analysis. Surface temperatures and other environmental measurements (e.g., surface salinity) were recorded using the ship's sensors interfaced with the ship's Scientific Computing System (SCS).

### Survey Design

The survey was designed with 26 north-south parallel transects that were either spaced 3 nmi apart or 6 nmi apart between about  $167^{\circ}\text{W}$  (Unalaska Island) and  $170^{\circ}\text{W}$  (Islands of Four Mountains). The wider 6 nmi spacing was strategic to conserve transecting time in areas where low pollock density was observed in 2016 and 2018, when 3 nmi transect spacing was used throughout the survey. The survey's start location was not randomized, and it started at the same location (longitude) as in 2018. For comparison purposes, the survey was divided into two regions, Umnak (transects 1-10), and Samalga (transects 11-26), according to differing pollock length distribution in these two areas during prior surveys. Survey operations were conducted from east to west 24 hours/day.

Trawl hauls were conducted to identify the species composition of observed acoustic scattering layers and to provide biological samples. Catches were sorted to species and weighed. Organism lengths were measured to the nearest 1 millimeter (mm) using an electronic measuring board (Towler and Williams 2010). A random subset of pollock were sampled to determine sex (for FL > 20 cm), fork length (FL), body weight, age, gonad maturity, and ovary weights. When the pollock sex ratio was dominated by one sex (e.g., 90% females), an additional subset of pollock were sampled (non-randomly) to represent the less dominant gender's FL, body weight, age, gonad maturity, and ovary weights. Smaller forage fishes such as lanternfishes (family Myctophidae) were measured to the nearest 1 mm standard length. An electronic motion-compensating scale (Marel M60) was used to weigh individual specimens to the nearest 2 g. Pollock otoliths were collected and stored in 50% glycerin/thymol-water solution for age determination by the AFSC Age and Growth Program researchers. Gonad maturity was determined by visual inspection and categorized as immature, developing, mature (hereafter, "pre-spawning"), spawning, or spent (hereafter, "post-spawning")<sup>3</sup>. Gonadosomatic indices (GSI) were computed as ovary weight/body weight for pre-spawning mature pollock. Trawl station and biological measurements were electronically recorded and stored using the Catch Logger for Acoustic Midwater Surveys (CLAMS) database. Each pocket net catch was logged separately, in a manner similar to, the codend catch.

Additional biological samples were collected for special projects. Pollock ovaries were collected from pre-spawning walleye pollock to investigate interannual variation in fecundity of mature females ([Sandi.Neidetcher@noaa.gov](mailto:Sandi.Neidetcher@noaa.gov)), and from female walleye pollock of all maturity stages for a histological study ([Martin.Dorn@noaa.gov](mailto:Martin.Dorn@noaa.gov)). Fin clips were taken from pollock to investigate the genetic population structure within spawning stocks ([Ingrid.Spies@noaa.gov](mailto:Ingrid.Spies@noaa.gov)), and gill tissue from pollock were collected for an evolutionary marker analysis (contact: Einar Arnason, [einararn@hi.is](mailto:einararn@hi.is), 354-525-4613, Iceland). Results from these special projects will be reported elsewhere.

---

<sup>3</sup> <https://repository.library.noaa.gov/view/noaa/50147>

## Data Analysis

### Processing acoustic data

Acoustic backscatter was classified into categories based on trawl catch information, frequency response (De Robertis et al. 2010), and by the backscatter appearance using Echoview software. Backscatter categories included near-surface unidentified, deep unidentified, pollock, fishes, lanternfishes, and euphausiids. Backscatter at 38 kHz in categories containing pollock was integrated at 0.5 nmi horizontal by 20 m vertical resolution, exported to a database, and converted to abundance and biomass using length and weight information. All other backscatter was excluded from analyses.

### From backscatter to abundance, an overview

Pollock acoustic backscatter was combined with trawl catch information to estimate pollock abundance. The analysis method had several principal steps. First, backscatter considered to contain pollock based on its appearance and vertical distribution on the echogram were assigned to the nearest geographical trawl catch and allocated to all scatterers from that catch. Second, a correction was made for net selectivity (based on relationships derived from the recapture nets; Williams et al. 2011). Third, backscatter was converted to estimates of abundance from the nearest-haul catch and the expected backscatter from each organism given species and size. Biomass was computed from abundance using the mean weight-at-length from random specimens in the survey. These steps are described in greater detail below and in Appendices III-IV and are an improvement over previous year's analyses in the Bogoslof area. In previous years (1988-2018), backscatter was allocated only to pollock, pollock length compositions from multiple hauls were often combined for regional representation (e.g., Samalga), and no net selectivity corrections were applied to any species.

### Selectivity correction

Previous research found that smaller fish are less likely to be retained in large midwater trawls than larger fish (Williams et al. 2011). To correct for this retention difference, trawl selectivity was estimated using recapture nets mounted on the LFS1421 midwater net (Appendix III). The counts and weights of animals caught in the recapture nets were expanded to provide an estimate

of escapement from the entire trawl. The catch of all species captured in the LFS1421 was corrected for the estimated probability of escapement by dividing the abundance of a given species and size class by the estimated probability of retention of that species and size class. Where the LFS1421 midwater net was used in analysis, LFS1421 selectivity corrections were made for pollock, lanternfish, other fish, squid, and non-krill crustacean species (Table A1). Where the AWT was used in analysis (haul 2), AWT selectivity correction for pollock was made. Except for when the AWT net was used in analysis, the 2020 primary analysis estimates include selectivity corrections for all organisms across the survey. This is the first year that any net-selectivity corrections were applied to estimates of abundance in the Bogoslof area.

#### Male-female ratio adjustment (equal-sex correction)

In the Bogoslof Island area, pre-spawning pollock aggregations are often densely packed and sometimes vertically stratified by sex, with males dominating the deeper pollock scattering layers and the females dominating the shallower layers (Honkalehto and Williamson 1995, Schabetsberger et al. 1999). The vertically stratified layers make it difficult to sample the deeper layers without over-sampling the shallower layer. Because female pollock > 5 years of age tend to be longer than males, over-sampling the shallower layer can lead to biased estimates of population proportion-at-length. Since 1994, the Bogoslof survey proportion-at-length estimates have been derived assuming that the true population's sex ratio was 50:50, rather than the sex ratio observed in the specimens collected in the trawl hauls (Honkalehto and Williamson 1995). For the Bogoslof Island survey estimates in years 1994-2018, the equal-sex correction was implemented to support the 50:50 sex ratio assumption.

For the 2020 survey analysis and final abundance estimates, proportion-at-length was not computed using the equal-sex correction. Instead, proportion-at-length estimates were based on pollock captured from the nearest geographical trawl catch that included net-selectivity corrections but without the equal-sex correction (Appendix IV). This change in analysis procedure was implemented to avoid combining correction procedures (i.e., equal-sex and net-selectivity), when deriving the population estimates.



### Abundance calculations

Fish abundance was calculated by combining species and size compositions from the hauls with acoustic backscatter data following the approach described in De Robertis et al. (2017) and in Appendix IV. A series of target strength (TS) to length relationships from the literature were used along with size and species distributions from LFS1421 trawl catches to estimate the proportion of the observed acoustic scattering attributable to each of the species captured in the trawls. For species for which the TS relationship was derived using a different length measurement type than the one used for measuring the trawl catch specimens, an appropriate length-length conversion was applied. For abundant species (e.g., contributing > 5% of the backscatter, an appropriate TS to length relationship available in the literature was used for that species. Other, less abundant taxa, were assigned to one of five generic categories: fishes with swim bladders, fishes without swim bladders, jellyfish, squid, and pelagic crustaceans (Table 2). In this survey, 97% of the backscatter was attributed to pollock so the species-specific TS to length relationship was applied, and generic TS to length relationships were used for all other species (Table 2).

Pollock mean weight-at-length was estimated using specimens from all trawl catches. For the primary analysis, weight-at-length measurements from randomly selected pollock specimens were used to estimate mean weight-at-length for each 1-cm length interval. When < 5 pollock occurred per interval, weight at a given length interval was estimated from a linear regression of the natural logs of the length and weight data and corrected for a small bias due to back-transformation (Miller 1984, De Robertis and Williams 2008; Appendix III). For analyses that implemented the equal-sex correction, non-random specimens were included to estimate the mean weight-at-length for each 1-cm length interval. The non-random fish were the additional male fish (or females) that were selected from the catch to supplement the length-weight and length-age samples in the analyses that implemented the equal-sex correction.

An age-length key from specimens in all trawl catches, and a subsequent proportion-at-age matrix, was applied to the population numbers-at-length and biomass-at-length to estimate numbers and biomass at age (Appendix III in Jones, et al. 2017; Appendix IV). For population

estimates at lengths where no otolith specimens were collected, the proportion-at-age was estimated using a Gaussian-model approach based on historical age-at-length data (1988-2020).

### Maturity data processing

Maturity data by haul were weighted by the local abundance of adult pollock (number of individuals > 30 cm FL). The 30 cm size criterion was selected as it represents the minimum size at which 5% of pollock are mature. The sum of the local abundance,  $A_h$ , assigned to the geographically nearest haul was computed. A weight,  $W_h$ , was then assigned to each haul by dividing the local haul abundance  $A_h$  by the average abundance per haul  $\bar{A}$ :

$$W_h = A_h / \bar{A} , \quad (\text{Eqn 1})$$

where

$$\bar{A} = \sum_h A_h / H , \quad (\text{Eqn 2})$$

and  $H$  is the total number of hauls.

The percent of pollock,  $PP_{sex,mat}$  greater than 30 cm FL by sex and maturity stage (immature, developing, pre-spawning, spawning, or spent) was computed for each haul and combined by survey area using a weighted average with  $W_h$ :

$$PP_{sex,mat} = \frac{\sum_h (N_{sex,mat,h} \cdot W_h)}{\sum_h W_h} , \quad (\text{Eqn 3})$$

where  $N_{(sex,mat,h)}$  is the number of pollock greater than 30 cm FL by sex and maturity for each haul.

For each haul, the number of female pollock considered mature (pre-spawning, spawning, or spent) and immature (immature or developing) were determined for each cm length bin. The length at 50% maturity (L50) was estimated for female pollock as a logistic regression using a

weighted generalized linear model following Williams 2007 with the inclusion of the haul weights,  $W_h$ , into the model (function `glm`, R Core Team, 2021).

The gonadosomatic index,  $GSI_h$ , [GSI: ovary weight/(total body weight)] was calculated for pre-spawning females in each haul and then a weighted average was computed for each survey area with  $W_h$ :

$$GSI = \frac{\sum_h (GSI_h \cdot W_h)}{\sum_h W_h} \quad (\text{Eqn 4})$$

The mean GSI for 2020 for Umnak and Samalga were compared to the mean GSI and standard deviation from historical years 2003-2018. For these historical surveys, the average-haul approach was used to estimate pollock abundance. Historically, the averaged-haul groupings usually represented a survey region. For example, a group of hauls averaged together might represent the pollock length composition for specific transects in the Umnak region and a different haul grouping would represent the length composition for transects in the Samalga region. Although the abundance estimates for historical surveys were not reanalyzed using the nearest haul approach, the nearest haul-interval assignments were used to identify the local abundance necessary for weighting the historical maturity data. Haul-interval assignments were constrained to match the same haul-transect relationship used in the original analyses. Intervals and transects that were geographically closest to the hauls used in the original analysis were identified, and the associated abundance were summed to represent the local abundance,  $A_h$ . For the historical surveys 2003, and 2005, the Umnak regions were subdivided by transect into the Unalaska and Umnak regions. For this analysis, the haul-weighted GSI was first computed for the Unalaska and Umnak regions separately, and then averaged to represent the Umnak region.

#### Pollock vertical distribution

Estimates of average pollock depth (weighted by biomass) were compared to the average bottom depth for each 0.5 nmi distance interval. Average pollock depth for each 0.5 nmi interval was computed as:

$$\text{average pollock depth} = \frac{\sum_D D*B}{\sum_D B} , \quad (\text{Eqn 5})$$

where D is the midpoint depth (m) of each 20 m depth layer, and B is biomass in the 20 m depth layer. Average bottom depth was the average sounder-detected bottom depth in each interval. The average pollock depth was sometimes deeper than the average sounder-detected bottom depth in areas of extreme slope. In these cases, the maximum depth of the pollock backscatter was used as the average bottom depth.

### Relative estimation error

In all areas, transects were parallel and relative estimation errors for the acoustic-based estimates were derived using a one-dimensional (1-D) geostatistical method (Petitgas 1993, Williamson and Traynor 1996, Walline 2007). “Relative estimation error” is defined as the ratio of the square root of the 1-D estimation variance ( $variance_{sum}$ ) to the biomass estimate (i.e., the sum of biomass over all transects,  $biomass_{sum}$ , kg):

$$\text{Relative estimation error}_{1-D} = \frac{\sqrt{variance_{sum}}}{biomass_{sum}} . \quad (\text{Eqn 6})$$

Because sampling resolution affects the variance estimate, and the 1-D method assumes equal transect spacing, estimation variance was determined separately in each area with unique transect spacing. Relative estimation error for an entire survey area (among  $n$  survey areas with different transect spacings) was computed by summing the estimation variance for each area  $j$ , taking the square root, and then dividing by the sum of the biomass over all areas, assuming independence among estimation errors for each survey area (Rivoirard et al. 2000):

$$\text{Relative estimation error}_{1-D \text{ survey}} = \frac{\sqrt{\sum_{j=1}^n variance_{sum_j}}}{\sum_{j=1}^n biomass_{sum_j}} . \quad (\text{Eqn 7})$$

Geostatistical methods were used to compute estimation error as a means to account for estimation uncertainty arising from the observed spatial structure in the fish distribution. These errors, however, quantify only transect sampling variability of the acoustic data (Rivoirard et al. 2000). Other sources of error (e.g., target strength, trawl sampling) were not evaluated.

### Sensitivity analysis

In addition to the primary analysis that produced the 2020 estimated abundance and biomass of pollock in the Bogoslof area (A-1), a sensitivity analysis was conducted to measure the effect of specific changes (e.g., net selectivity) implemented in 2020 as compared to analysis methods implemented in previous years. As a reminder, the 2020 primary analysis (A-1) implemented the 1) single nearest-haul approach that accounted for all species in the catch, 2) net-selectivity corrections, but 3) no equal-sex corrections. Previous survey analyses (historical: 1988-2018) allocated backscatter only to pollock rather than accounting for all species, and often combined pollock length compositions from different hauls to obtain a pollock length composition that represented an area (i.e., Samalga). While no net-selectivity corrections were applied in previous survey analyses, some analyses did implement the equal-sex correction (1994-2018).

The sensitivity analysis measured the effect of specific changes to the primary analysis, A-1, which are italicized in A-3 and A-9 below, and compares the A-1 results with results using the historical methods (A-2) and variations of the historical methods (A-8, A-12).

- Pooled pollock lengths from multiple hauls, backscatter allocated only to pollock, no net-selectivity correction, with equal-sex correction (A-2)
- Single nearest-haul pollock lengths, backscatter allocated to all species, *no net-selectivity correction, with equal-sex correction* (A-3)
- Pooled pollock lengths from multiple hauls, backscatter allocated only to pollock, no net-selectivity correction, no equal-sex correction (A-8)
- Single nearest-haul pollock lengths, backscatter allocated to all species, *no net-selectivity correction, no equal-sex correction* (A-9)

- Pooled pollock lengths from multiple hauls, backscatter allocated only to pollock, with net-selectivity (pollock only) correction, no equal-sex correction (A-12)

## **RESULTS AND DISCUSSION**

### Survey Weather Detours

Poor weather conditions detoured the originally planned survey operations. At the start of the cruise, the weather and sea conditions were unfavorable for transiting from Sand Point, Alaska (Appendix I) to the Bogoslof survey area, so the ship stayed in the area and conducted a requested trawl sample in the Shumagin Islands area for the DY2020-01 survey effort. After which, the ship transited to the Bogoslof survey area to begin the survey. Weather also limited backscatter sampling with both nets (paired trawling LFS1421-AWT), and in many cases only one net was used to sample backscatter. After finishing the survey lines, weather forced the ship to shelter 12.5 hours in Nikolski Bay, effectively cancelling further trawl sampling in the Bogoslof area. The ship then proceeded back to Shelikof Strait, where calmer sea conditions allowed for paired-trawl sampling for cruise DY2020-03.

### Calibration

Pre- and post-survey calibration measurements of the 38 kHz echosounder showed no significant differences in gain parameters or beam pattern characteristics, confirming that the acoustic system was stable throughout the survey (Table 1). At 38 kHz the echo integration gain differed by  $< 0.05$  dB across the two measurements, and the average of all calibration results (averages calculated in the linear domain for dB quantities) were used in the final analysis (Table 1). Nominal sound speed and absorption values appropriate for the survey areas were used in the final parameter set, and the equivalent beam angle was adjusted (Bodholt 2002) using the sound speed assumed during survey conditions for data analysis.

### Survey Coverage

The survey covered 1,449 nmi<sup>2</sup> of the CBS Convention Specific Area (Fig. 1). Acoustic backscatter at 38 kHz was measured along 26 tracklines totaling 671 km (362.4 nmi).

### Water Temperature

Water temperatures measured during the 2020 survey were cooler than temperatures measured in 2018. Mean surface temperatures ranged from 3.6 ° to 4.6 °C in 2020 (Fig. 2), whereas mean surface temperatures ranged from 4.1 ° to 4.7 °C in 2018. The coolest surface temperatures measured in 2020 were observed in the westernmost transect, which was different than in 2018, when the coolest temperatures were observed in the eastern most transects. Water temperatures at trawl sites were measured to a maximum depth of 396 m, and were cooler in the upper 300 m compared to 2018 (Fig. 3). Temperatures between 250 and 400 m, the depth range where most of the pollock were distributed in the Bogoslof area in 2020, averaged 4.2 °C in 2020, which was the same temperature average in 2018 for the same depth range (Fig. 3). When compared to temperature profiles observed from previous Bogoslof surveys, the profile in 2020 was cooler than 2016 (the warmest year in the time series between 2000 and 2020).

### Trawl Samples

Biological data and specimens were collected from 1 trawl location in the Shumagin Islands, 14 trawl locations in the Bogoslof Island area, and 2 trawl locations in Shelikof Strait (Table 3). Only biological data from samples collected in the Bogoslof area will be summarized in this report.

Although paired hauls using the LFS1421 and AWT nets sampled the same backscatter at multiple locations for the trawl comparison study, catch data from the LFS1421 were the primary biological data source for this survey analysis. On one occasion however, the AWT sample was used in place of the LFS1421 catch because the LFS1421 trawl fouled (haul 1).

Pollock dominated the trawl catches in both midwater nets by weight and number, representing 99.2% of the total catch by weight for the 6 AWT hauls (Table 4), and 96.8% of the total catch

by weight for the 8 LFS1421 hauls (Table 5). Lanternfishes were the second most numerous species captured in the AWT hauls (8.8%), whereas shrimp species were the second most numerous species captured in the LFS1421 hauls (14.9%). Comparison of the length frequency of pollock between the LFS1421 and AWT trawl hauls suggested that catch of the two nets is very similar, differing mainly in retention of small organisms; the proportion of pollock captured at length does not differ appreciably between the LFS1421 and AWT nets. The results of the trawl comparison study will be reported in detail elsewhere (Williams and Kotwicki, in preparation).

Pollock random length measurements used in the abundance estimates came from LFS1421 hauls 3, 5-6, 9-10, 13-14, and from AWT haul 2 (Table 6,  $n = 2,350$ ). Pollock length measurements in the Umnak area (hauls 2-3, 5-6) were bimodal and had a broader range of lengths compared to the Samalga samples from hauls 9-10, 13-14 (Fig. 4). Overall, fish lengths ranged from 29 to 69 cm FL, with a primary mode at 53 cm fork length (FL). Of these length measurements, 73% of the length measurements were from female pollock and 27% were male pollock.

Pollock specimens ( $> 30$  cm FL, random) were examined for maturity stages and the weighted maturity-compositions were different in the Umnak and the Samalga regions. In the Umnak region, of the 226 females, 5% were immature, 36% were developing, 41% were in the pre-spawning stage, 11% were spawning, and 7% were in the post-spawning stage (Fig. 5a, Umnak). Of the 92 males, 10% were immature, 21% were developing, 11% were pre-spawning, 57% were spawning, and 1% were in the post-spawning stage. In the Samalga region, of the 168 females, 0% were immature, 0% were developing, 99% were in the pre-spawning stage, 1% were spawning, and 0% were in the post-spawning stage (Fig. 5a, Samalga). Of the 68 males, 0% were immature, 2% were developing, 29% were in the pre-spawning stage, 69% were spawning, and 0% were in the post-spawning stage.



The length at which 50% of female pollock > 30 cm FL were determined to be reproductively mature (i.e., pre-spawning, spawning, or spent) was 47.4 cm FL in the Umnak region (Fig. 5b-Umnak). L50 could not be accurately estimated for the Samalga region because the female pollock specimens were nearly all were reproductively mature, and therefore, a lack of contrast in length and maturity status. The overall average gonadosomatic index (GSI) for pre-spawning mature female pollock observed in 2020 was 0.16. By region, the GSI was  $0.15 \pm 0.026$  in Umnak (Fig. 5c-Umnak), which was lower than the estimated abundance-weighted GSI in 2018 (i.e., 0.17), yet within the historical standard deviation for GSI in the Umnak region. Whereas the GSI in the Samalga region was  $0.18 \pm 0.004$ , which exceeded the historical mean and standard deviation (Fig. 5c-Samalga).

#### Distribution and Abundance

Pollock biomass was distributed on all transects with 12% of the biomass distributed in the Umnak region (transects 1-10), and 88% of the biomass distributed in the Samalga region (Fig. 6). The densest concentration was located on transect 22, within the Samalga region, which represented 44% of the estimated pollock biomass. This layer extended horizontally for about 7.5 nmi with a vertical extent from 260 m down to 600 m below the surface.

Pollock biomass-weighted depth estimates ranged from about 100 to 600 m for the entire surveyed area (Fig. 7). Fish generally stayed close to the bottom until bottom depths reached about 300 m. Pollock formed pelagic layers around 300-500 m over deeper bottom depths (> 600 m). The pollock mean biomass-weighted depth estimate was 355 m for the Umnak area and 384 m for the Samalga area. The pollock biomass-weighted depth estimate for the dense aggregation on transect 22 was 374 m.

The pollock abundance estimate in 2020 was 338 million fish weighing 353 thousand metric tons for the entire surveyed area (Tables 7-9). The overall size composition for the pollock was unimodal at about 53 cm FL (Fig. 8), with an average length at 52.5 cm (Table 8). The estimates represent a 65% decrease in abundance and a 47% decrease in biomass from the 2018 survey estimates of 964 million fish weighing 663 thousand metric tons (McKelvey and Levine 2018;

Tables 7-8, Figs. 8-10). Based on the 1D geostatistical analysis, the relative estimation error for the biomass estimate was 15.8% (Table 7).

The estimated age composition for pollock ranged from 2 to 14 years of age (Tables 10-11; Fig. 11). Sixty-one percent of the estimated biomass were 10-11-year old fish (2010-2009 year classes), and another 16% were 9-year-old fish from the 2011 year class (Fig.11-12). Numerous 3 year old pollock were sampled during the 2020 survey, primarily from the Umnak region. Walleye pollock aged 12-13 years were smaller than historical lengths-at-age observed 2003-2018 (Fig. 13).

### Sensitivity Analysis

Results from the sensitivity analysis showed that the 2020 abundance and biomass varied from the primary A-1 analysis depending on the alternative analysis method and correction applied (Table 12, Fig. 14). In comparing the A-1 analysis with the other nearest-haul variations (A-3, A-9), we see minor changes in biomass ( $\pm 1\%$ ) and more variable changes in abundance (+ 1-5%). For example, only + 1% change in abundance and biomass was observed if net-selectivity was not implemented (A-9); given that few juvenile pollock are historically captured in the Bogoslof region (pollock were  $> 29$  cm FL in 2020), it is likely that the net-selectivity correction mostly affected non-pollock species (e.g., myctophids) in the primary analysis, so when it was not applied (A-9), less backscatter was allocated to smaller species in the catches thereby increasing the backscatter allocated to pollock. If an equal-sex correction was implemented (A-3), the abundance increased 5% and the biomass decreased 1%, because more backscatter was allocated to smaller, more numerous male pollock. In 2020, the pollock female to male ratio (weighted average) was about 4:1 in the trawl catches, but with the equal-sex correction, more emphasis was given to male pollock, shifting the mode of all pollock from 53 cm to 50 cm FL, thereby increasing the abundance and reducing the biomass.

By comparing results from the primary A-1 analysis with the historical approach analyses (A-2, A-8, A-12), where backscatter was allocated only to pollock, and pollock lengths were pooled to represent regions, we see increases in abundance and biomass in the historical approach,

depending on the additional corrections implemented. The largest increase in abundance (7%) was observed in A-2, which included an equal-sex correction, but no net-selectivity correction; whereas, the largest biomass increase (3.4%) was observed in A-8 (no equal-sex or net-selectivity corrections) and A-12 (no equal-sex correction, but net-selectivity correction was made). In comparing between historical approaches A-8 and A-12 (without and with the net-selectivity correction), we see that pollock net-selectivity had no effect. But in comparing A-2 with A-8 (with and without the equal-sex correction), we see an increase in biomass when more backscatter was allocated to larger female pollock.

### Survey Time Series and Future Directions

The 2020 Bogoslof acoustic-trawl survey for pollock began 2 weeks earlier than the survey conducted in 2018, and earlier than many other past surveys (Table 13, Fig. 15). This timing shifted earlier because of vessel scheduling constraints, and because the 2016-2018 survey results showed that female pollock were well past peak spawning (Table 13). In contrast to the 2016-2018 surveys, relatively few of the 2020 female pollock were in spawning or post-spawning maturity stages (1.2% Samalga, 13.4% Umnak; unweighted values are used in Table 13 for comparison with past surveys), indicating that most of the female pollock were in a maturity state that was appropriate for this pre-spawning survey and consistent with a majority of past surveys. Weighted spawning and post-spawning maturity percentages for 2020 female pollock lead to the same conclusion (1.0% Samalga, 18.0% Umnak). While the survey timing in 2020 was appropriate, it might be difficult to optimize survey timing in the future. Thus, further analyses of the Bogoslof survey time series is warranted to determine if the late-maturity stages is an indicator of pollock leaving the survey area after spawning resulting in a survey abundance with a negative bias (Wilson 1994), and to determine whether the percent of fish in spawning and post-spawning condition can be predicted based on factors such as calendar date, population size, average fish length, location, or environmental conditions (Lawson and Rose 2000).

Improvements in the gear and analysis methods marks the 2020 survey results. This was the first survey in the Bogoslof time series that the LFS1421 net was used as the primary sampling tool and net-selectivity corrections were applied. Additionally, this was the first survey in the time

series that the analysis changed to implement the nearest-haul methodology. Historically during analysis, pollock length compositions from multiple trawl catches were pooled, and then the averaged lengths were applied to intervals within a region. While the older approach averaged out the variability in pollock lengths from trawl to trawl, applying length composition from the nearest individual haul to scale intervals allows for complex computations that improve the estimates. Improvements include allocating backscatter to all species in the trawl rather than assuming pollock were the only species contributing to the backscatter. The nearest-haul approach also provides a mechanism to compute an abundance-weighted maturity composition that describes the maturity profile for the entire fish population. Although the nearest-haul assignment is currently automated, the process requires some supervision to avoid haul assignments to distant intervals or unreasonable interval assignments due to clustered net samples (e.g., Samalga region).

The 2020 survey also changed the analysis to no longer assume a 50:50 sex ratio in the Bogoslof pollock population as it had in previous surveys (1994-2018). Instead, the 2020 analysis relied on net catches without equal-sex corrections to scale the acoustic backscatter. With the poor weather conditions during the 2020 survey in the Bogoslof region, we were unable to sample in the deep waters, where male pollock often stratify. Thus, it is possible that more males were present in the population but were underrepresented in the pollock abundance and biomass estimates. Future surveys need to sample the deep and shallow backscatter layers multiple times using a closed codend to determine whether pre-spawning pollock continue to vertically stratify by sex in the Bogoslof region. Additional samples using the open-codend trawl equipped with the stereo camera system offer another tool to examine whether vertical stratification persists. Camera images have potential to observe whether fish in the deeper layers are shorter in length than the fish in the shallower layers, while avoiding filling the net with fish from the shallower layers.

## ACKNOWLEDGMENTS

The authors would like to thank the officers and crew of the NOAA ship *Oscar Dyson*, and all of the scientists who prepared for and participated in this survey for their contributions to the successful completion of this work.



## CITATIONS

- Bodholt, H., 2002. The effect of water temperature and salinity on echo sounder measurements. ICES Symposium on Acoustics in Fisheries, Montpellier 10–14 June 2002.
- Demer, D. A., and S. G. Conti. 2005. New target-strength model indicates more krill in the Southern Ocean. ICES J. Mar. Sci. 62: 25-32.
- Demer, D. A., L.N. Andersen, C. Bassett, L. Berger, D. Chu, J. Condiotty, G.R. Cutter, B. Hutton, R. Korneliussen, N. Le Bouffant, G. Macaulay, W.L. Michaels, D. Murfin, A. Pobitzer, J.S. Renfree, T.S. Sessions, K.L. Stierhoff, and C.H. Thompson. 2017. 2016 USA–Norway EK80 Workshop Report: Evaluation of a wideband echosounder for fisheries and marine ecosystem science. ICES Coop. Res. Rep. 336. 69 p.
- De Robertis, A., D. R. McKelvey, and P. H. Ressler. 2010. Development and application of an empirical multifrequency method for backscatter classification. Can. J. Fish. Aquat. Sci. 67:1459-1474.
- De Robertis, A., and K. Taylor. 2014. *In situ* target strength measurements of the scyphomedusa *Chrysaora melanaster*. Fish. Res. 153:18-23.
- De Robertis, A., K. Taylor, C.D. Wilson, and E. V. Farley. 2017. Abundance and distribution of Arctic cod (*Boreogadus saida*) and other pelagic fishes over the U.S. continental shelf of the northern Bering and Chukchi seas. Deep-Sea Res. II. 135: 51-65.3
- De Robertis, A., and K. Williams. 2008. Weight-length relationships in fisheries studies: the standard allometric model should be applied with caution. Trans. Am. Fish. Soc. 137:707–719.

- Foote, K.G. 1987. Fish target strengths for use in echo integration surveys. J. Acoust. Soc. Am. 82: 981-987.
- Foote, K. G., H. P. Knudsen, G. Vestnes, D. N. MacLennan, and E. J. Simmonds. 1987. Calibration of acoustic instruments for fish density estimation: a practical guide. ICES Coop. Res. Rep. 144, 69 p.
- Foote, K. G., and J. Traynor. 1988. Comparison of walleye pollock target-strength estimates determined from *in situ* measurements and calculations based on swimbladder form. J. Acoust. Soc. Am. 83: 9-17.
- Gauthier, S., and J. K. Horne. 2004. Acoustic characteristics of forage fish species in the Gulf of Alaska and Bering Sea. Can. J. Fish. Aquat. Sci. 61: 1839-1850.
- Honkalehto, T., and N. Williamson. 1995. Echo integration-trawl survey of walleye pollock (*Theragra chalcogramma*) in the southeast Aleutian Basin during February and March, 1994. U.S. Dep. Commer., NOAA Tech. Memo. NMFS-AFSC-52, 39 p.
- Honkalehto, T., D. McKelvey, and K. Williams. 2008. Results of the March 2007 echo integration-trawl survey of walleye pollock (*Theragra chalcogramma*) conducted in the southeastern Aleutian Basin near Bogoslof Island, cruise MF2007-03. AFSC Processed Rep. 2008-01, 37 p. Alaska Fish. Sci. Cent., Natl. Mar. Fish. Serv., NOAA, 7600 Sand Point Way NE., Seattle WA 98115.
- Ianelli, J. N., S. J. Barbeaux, and D. McKelvey. 2020. Assessment of walleye pollock in the Bogoslof Island Region. *In* Stock assessment and fishery evaluation report for the groundfish resources of the Bering Sea/Aleutian Islands regions. N. Pac. Fish. Mgmt. Council, 605 W. 4<sup>th</sup> Ave, Anchorage, AK 99501-2252.



- Jech, J. M., K. G. Foote, Chu, D., L. C. Hufnagle, 2005. Comparing two 38-kHz scientific echosounders. *ICES J. Mar. Sci.* 62, 1168-1179.
- Jones, D. T., A. De Robertis, and N. J. Williamson. 2011. Statistical combination of multifrequency sounder-detected bottom lines reduces bottom integrations. U.S. Dep. Commer., NOAA Tech. Memo. NMFS-AFSC-219, 13 p.
- Jones, D. T., S. Stienessen, and N. Lauffenburger. 2017. Results of the acoustic-trawl survey of walleye pollock (*Gadus chalcogrammus*) in the Gulf of Alaska, June-August 2015 (DY2015-06). AFSC Processed Rep. 2017-03, 102 p. Alaska Fish. Sci. Cent., NOAA, Natl. Mar. Fish. Serv., 7600 Sand Point Way NE., Seattle WA 98115.
- Kang, D., T. Mukai, K. Iida, D. Hwang, and J.-G. Myoung. 2005. The influence of tilt angle on the acoustic target strength of the Japanese common squid (*Todarodes pacificus*). *ICES J. Mar. Sci.* 62: 779-789.
- Lawson, G. L., and G.A. Rose. 2000. Small-scale spatial and temporal patterns in spawning of Atlantic cod (*Gadus morhua*) in coastal Newfoundland waters. *Can. J. Fish. Aquat. Sci.* 57:1011-1024.
- McKelvey, D., and M. Levine. 2018. Results of the March 2018 acoustic-trawl survey of walleye pollock (*Gadus chalcogrammus*) conducted in the Southeastern Aleutian Basin near Bogoslof Island, Cruise DY2018-02. AFSC Processed Rep. 2018-07, 44 p. Alaska Fish. Sci. Cent., Natl. Mar. Fish. Serv., NOAA, 7600 Sand Point Way NE., Seattle WA 98115.
- MacLennan, D. N., P. G. Fernandes, and J. Dalen. 2002. A consistent approach to definitions and symbols in fisheries acoustics. *ICES J. Mar. Sci.* 59:365-369.
- Miller, D. M. 1984. Reducing transformation bias in curve fitting. *Am. Stat.* 38:124-126.

- Petitgas, P. 1993. Geostatistics for fish stock assessments: a review and an acoustic application. ICES J. Mar. Sci. 50: 285-298.
- Rivoirard, J., J. Simmonds, K.G. Foote, P. Fernandez, and N. Bez. 2000. Geostatistics for estimating fish abundance. Blackwell Science Ltd., Osney Mead, Oxford OX2 0EL, England. 206 p.
- Schabetsberger, R., R. D. Brodeur, T. Honkalehto, and K. L. Mier. 1999. Sex-biased cannibalism in spawning walleye pollock: the role of reproductive behavior. Environ. Biol. Fishes 54:175-190.
- Simrad. 2018. EK80 scientific echo sounder software reference manual. 848 p. Simrad AS, Strandpromenenaden 50, 3183 Horten, Norway.
- Towler, R., and K. Williams. 2010. An inexpensive millimeter-accuracy electronic length measuring board. Fish. Res. 106:107-111.
- Traynor, J. J. 1996. Target strength measurements of walleye pollock (*Theragra chalcogramma*) and Pacific whiting (*Merluccius productus*). ICES J. Mar. Sci. 64:559-569.
- Walline, P. D. 2007. Geostatistical simulations of eastern Bering Sea walleye pollock spatial distributions, to estimate sampling precision. ICES J. Mar. Sci. 64:559-569.
- Williams, K., R. Towler, and C. Wilson. 2010. Cam-Trawl: A combination trawl and stereo-camera system. Sea Technol. 51(12).
- Williams, K., A. E. Punt, C. D. Wilson, and J. K. Horne. 2011. Length-selective retention of walleye pollock, *Theragra chalcogramma*, by midwater trawls. ICES J. Mar. Sci. 68:119-129.

- Williams, K. 2007. Evaluation of the macroscopic staging method for determining maturity of female walleye pollock *Theragra chalcogramma* in Shelikof Strait, Alaska. Alaska Fish. Res. Bull., 12: 252-263.
- Williams, K. and S. Kotwicki. *In prep.* Midwater trawl comparison study for acoustic surveys of walleye pollock (*Gadus chalcogrammus*) in Alaska. U.S. Dep. Commer., NOAA Tech. Memo.
- Williamson, N., and J. Traynor. 1996. Application of a one-dimensional geostatistical procedure to fisheries acoustic surveys of Alaskan pollock. ICES J. Mar. Sci. 53: 423-428.
- Wilson, C. D. 1994. Echo integration-trawl survey of pollock in Shelikof Strait Alaska in 1994, p. 1-39. *In* Stock Assessment and Fishery Evaluation Report for the 1994 Gulf of Alaska Groundfish Fishery, November 1994. Prepared by the Gulf of Alaska Groundfish Plan Team, North Pacific Fishery Management Council, P.O. Box 103136, Anchorage, AK 99510.

Table 1. -- Simrad EK80 38 kHz acoustic system description and settings used during the winter 2020 Gulf of Alaska acoustic-trawl surveys of walleye pollock. These include environmental parameters and results from standard sphere acoustic system calibrations conducted in association with the survey and final values used to calculate biomass & abundance data. The system settings column contains 12 February EK80 calibration utility results. Other columns are a combination of on-axis and EK80 calibration utility results (see Methods and Results and Discussion sections of text for details).

	Winter 2020 system settings	12 Feb Uganik Bay Alaska	16 Mar Kalsin Bay Alaska	Final analysis parameters
Echosounder	Simrad EK80	--	--	Simrad EK80
Transducer	ES38-7 s/n 324	--	--	ES38-7 s/n 324
Frequency (kHz)	38	--	--	38
Transducer depth (m)	9.15	--	--	9.15
Pulse length (ms)	1.024	--	--	1.024
Transmitted power (W)	2000	--	--	2000
Angle sensitivity along	18.00	--	--	18.00
Angle sensitivity athwart	18.00	--	--	18.00
2-way beam angle (dB re 1 steradian)	-20.70	--	--	-20.52
Gain (dB)	27.18	27.13	27.17	27.15
$s_A$ correction (dB)	-0.04	-0.05	-0.05	-0.05
Integration gain (dB)	27.14	27.08	27.12	27.10
3 dB beamwidth along	6.35	6.35	6.40	6.38
3 dB beamwidth athwart	6.44	6.44	6.46	6.45
Angle offset along	-0.04	-0.04	-0.04	-0.04
Angle offset athwart	0.06	0.06	0.06	0.06
Post-processing $S_v$ threshold (dB re 1 m <sup>-1</sup> )	-70	NA	NA	-70
Standard sphere TS (dB re 1 m <sup>2</sup> )	NA	-42.15	-42.13	NA
Sphere range from transducer (m)	NA	20.27	20.78	NA
Absorption coefficient (dB/m)	0.0099	0.0099	0.0098	0.0099
Sound velocity (m/s)	1466.0	1460.5	1460.5	1466.0
Water temp at transducer (°C)	NA	3.8	3.3	NA

Note: Gain and beam pattern terms are defined in the Operator Manual for Simrad ER60 Scientific echosounder application, which is available from Simrad Strandpromenaden 50, Box 111, N-3191 Horten, Norway. -- symbol indicates the same values for the system settings and final analysis are also applicable for the various calibrations. NA indicates 'not applicable'.

Table 2 -- Target strength (TS) to size relationships from the literature used to allocate 38 kHz acoustic backscatter to most species in this report. The symbols in the equations are as follows: r is the bell radius in cm and L is length in cm for all groups except pelagic crustaceans, in which case L is in millimeters.

Group	TS (dB re 1 m <sup>2</sup> )	Length type	TS derived for which species	Reference
Walleye pollock	$TS = 20 \log_{10} L - 66$	L = fork length	<i>Gadus chalcogrammus</i>	Foote & Traynor (1988), Traynor (1996)
Pacific capelin	$TS = 20 \log_{10} L - 70.3$	L = total length	<i>Mallotus catervarius</i>	Guttormsen and Wilson (2009)
Pacific herring	$TS = 20 \log_{10} L - 2.3 \log_{10}(1 + depth/10) - 65.4$	L = fork length	<i>Clupea harengus</i>	Ona (2003)
Fish with swim bladders	$TS = 20 \log_{10} L - 67.4$	L = total length	Physoclist fishes	Foote et al. (1987)
Fish without swim bladders	$TS = 20 \log_{10} L - 83.2$	L = total length	<i>Pleurogrammus monopterygius</i>	Gauthier & Horne (2004)
Jellyfish	$TS = 10 \log_{10}(\pi r^2) - 86.8$	r = bell radius	<i>Chrysaora melanaster</i>	De Robertis & Taylor (2014)
Squid	$TS = 20 \log_{10} L - 75.4$	L = mantle length	<i>Todarodes pacificus</i>	Kang et al. (2005)
Eulachon	$TS = 20 \log_{10} L - 84.5$	L = total length	<i>Thaleichthys pacificus</i>	Gauthier and Horne (2004)
Pelagic crustaceans <sup>1</sup>	$TS = A * (\log_{10}(BkL)/(BkL))^c + D((kL)^6) + E((kL)^5) + F((kL)^4) + G((kL)^3) + H((kL)^2) + I(kL) + J + 20 \log_{10}(L/L_0)$	L = total length	<i>Euphausia superba</i>	Demer & Conti (2005)

<sup>1</sup>A = -930.429983; B = 3.21027896; C = 1.74003785; D = 1.36133896 x 10<sup>-8</sup>; E = -2.26958555 x 10<sup>-6</sup>  
F = 1.50291244 x 10<sup>-4</sup>; G = -4.86306872 x 10<sup>-3</sup>; H = 0.0738748423; I = -0.408004891; J = -73.9078690; and L<sub>0</sub> = 0.03835  
If L < 15 mm, TS = -105 dB; and if L > 65 mm, TS = -73 dB.  
k = 2πfc, where f = 38,000 (frequency in Hz) and c = 1470 (sound speed in m/s).

Table 3. – Trawl stations and catch data summaries from areas sampled during the winter 2020 acoustic-trawl survey of walleye pollock in the Bogoslof Island region.

Haul No.	Area	Gear Type <sup>a</sup>	Date (GMT)	Time (GMT)	Duration (mins)	Start Position		Depth (m)		Temp (C)		Walleye pollock		Other (kg)
						Lat. (N)	Long. (W)	Footrope <sup>b</sup>	Bottom	Headrope	Surface <sup>c</sup>	(kg)	Number	
5	Shumagin Islands	LFS1421	18-Feb	15:41	55.6	55.4636	-160.4805	112	149	-	3.3	249.9	320	1.2
1	Bogoslof	LFS1421	19-Feb	21:30	7.0	53.7085	-167.3656	340	381	4.2	4.1	7.7	9	1.9
2	Bogoslof	AWT	20-Feb	00:23	15.4	53.7103	-167.3639	367	354	4.3	4.1	180.8	378	10.9
3	Bogoslof	LFS1421	20-Feb	06:11	25.2	53.5983	-167.6202	331	546	-	4.3	334.8	505	20.1
4	Bogoslof	AWT	21-Feb	04:31	1.8	53.5773	-167.7953	376	736	4.2	4.1	6,377.5	5,958	13.5
5	Bogoslof	LFS1421	21-Feb	07:51	2.2	53.5809	-167.8050	277	766	4.4	4.2	123.3	127	3.7
6	Bogoslof	LFS1421	21-Feb	11:18	1.8	53.5797	-167.8763	277	387	4.4	4.1	572.9	578	12.1
7	Bogoslof	AWT	21-Feb	14:22	4.0	53.5794	-167.8752	284	376	4.4	4.1	1,389.0	1,370	41.0
8	Bogoslof	AWT	22-Feb	09:30	8.0	53.0846	-169.0372	297	377	4.3	4.3	784.1	544	4.6
9	Bogoslof	LFS1421	22-Feb	12:42	33.6	53.0911	-169.0413	330	451	4.0	4.2	393.5	321	8.3
10	Bogoslof	LFS1421	22-Feb	20:43	0.8	53.1410	-169.1269	366	960	4.1	4.2	1,439.6	1,316	62.4
11	Bogoslof	AWT	22-Feb	23:59	5.0	53.1374	-169.1247	404	883	3.9	4.3	339.8	313	2.9
12	Bogoslof	AWT	23-Feb	03:41	4.3	53.1260	-169.1230	380	796	4.2	4.3	93.3	101	4.0
13	Bogoslof	LFS1421	23-Feb	07:01	18.3	53.1252	-169.1304	398	778	4.2	4.2	584.4	546	9.7
14	Bogoslof	LFS1421	23-Feb	09:29	3.6	53.0931	-169.1330	340	705	4.0	4.2	284.0	258	3.6
15	Shelikof Strait	AWT	27-Feb	17:38	5.0	57.8625	-153.9592	184	198	5.6	4.7	357.2	887	725.3
16	Shelikof Strait	LFS1421	27-Feb	20:29	9.8	57.8673	-153.9527	176	199	5.7	4.4	256.2	763	947.1

<sup>a</sup>LFS1421 = LFS1421 midwater trawl, AWT = Aleutian Wing Trawl

<sup>b</sup>Footrope depth not collected on all trawls

<sup>c</sup>Average temperature measured from an SBE temperature logger

Table 4. -- Catch by species and numbers of length and weight measurements taken from individuals found in the codend during the 6 AWT hauls from the winter 2020 acoustic-trawl survey of walleye pollock in Bogoslof. Recapture net catch data are not included.

Species name	Scientific name	Catch				Measurements	
		Weight (kg)	%	Number	%	Length	Weight
walleye pollock	<i>Gadus chalcogrammus</i>	9,164.5	99.2	8,664	77.0	1,555	78
Pacific ocean perch	<i>Sebastes alutus</i>	44.6	0.5	54	0.5	5	3
lanternfish	<i>Stenobrachius</i> sp.	8.0	<0.1	947	8.4	143	10
smooth lumpsucker	<i>Aptocyclus ventricosus</i>	5.4	<0.1	3	<0.1	3	-
squid unid.	Cephalopoda (class)	4.4	<0.1	177	1.6	30	7
jellyfish	<i>Aequorea</i> sp.	3.5	<0.1	21	0.2	-	-
lamprey unid.	Petromyzontidae (family)	3.2	<0.1	8	<0.1	5	4
northern sea nettle	<i>Chrysaora melanaster</i>	1.8	<0.1	6	<0.1	3	2
northern smoothtongue	<i>Leuroglossus schmidti</i>	1.7	<0.1	886	7.9	36	-
brokenline lampfish	<i>Lampanyctus jordani</i>	1.6	<0.1	45	0.4	10	9
arrowtooth flounder	<i>Atheresthes stomias</i>	1.3	<0.1	1	<0.1	1	-
flathead sole	<i>Hippoglossoides elassodon</i>	0.7	<0.1	1	<0.1	1	-
shrimp unid.	Malacostraca (class)	0.4	<0.1	323	2.9	13	-
longnose lancetfish	<i>Alepisaurus ferox</i>	0.3	<0.1	10	<0.1	3	2
magistrate armhook squid	<i>Berryteuthis magister</i>	0.2	<0.1	1	<0.1	1	-
Hydromedusa (unid.)	Hydromedusa (unid.)	<0.1	<0.1	58	0.5	16	-
Pacific glass shrimp	<i>Pasiphaea pacifica</i>	<0.1	<0.1	35	0.3	6	-
helmet jelly	<i>Periphylla periphylla</i>	<0.1	<0.1	4	<0.1	4	-
blackmouth eelpout	<i>Lycodapus fierasfer</i>	<0.1	<0.1	5	<0.1	-	-
isopod unid.	Isopoda (order)	<0.1	<0.1	3	<0.1	-	-
Total		9,241.5		11,252		1,835	115

Table 5. -- Catch by species and numbers of length and weight measurements from individuals found in the codend during the 8 LFS1421 hauls from the winter 2020 acoustic-trawl survey of walleye pollock in Bogoslof. Recapture net catch data are not included.

Species name	Scientific name	Catch				Measurements	
		Weight (kg)	%	Number	%	Length	Weight
walleye pollock	<i>Gadus chalcogrammus</i>	3,740.3	96.8	3,660	56.2	2,059	564
smooth lump sucker	<i>Aptocyclus ventricosus</i>	60.3	1.6	36	0.6	4	4
Pacific ocean perch	<i>Sebastes alutus</i>	32.2	0.8	41	0.6	40	32
salmon unid.	<i>Oncorhynchus</i> (genus)	8.6	0.2	67	1.0	32	17
lanternfish	<i>Stenobrachius</i> sp.	4.4	0.1	626	9.6	159	77
jellyfish	<i>Aequorea</i> sp.	2.3	<0.1	16	0.2	1	1
chinook salmon	<i>Oncorhynchus tshawytscha</i>	1.8	<0.1	1	<0.1	1	1
squid unid.	Cephalopoda (class)	1.6	<0.1	279	4.3	18	8
northern smooth tongue	<i>Leuroglossus schmidti</i>	1.6	<0.1	626	9.6	75	26
egg yolk jelly	<i>Phacellophora camtschatica</i>	1.6	<0.1	2	<0.1	2	2
northern sea nettle	<i>Chrysaora melanaster</i>	1.3	<0.1	6	<0.1	5	5
lamprey unid.	Petromyzontidae (family)	1.0	<0.1	3	<0.1	3	3
jellyfish unid.	Scyphozoa (class)	0.9	<0.1	-	-	-	-
shrimp unid.	Malacostraca (class)	0.7	<0.1	826	12.7	25	6
euphausiid unid.	Euphausiacea (order)	0.7	<0.1	-	-	-	-
magistrate armhook squid	<i>Berryteuthis magister</i>	0.6	<0.1	6	<0.1	6	6
Pacific lamprey	<i>Lampetra tridentata</i>	0.6	<0.1	1	<0.1	1	1
Pelagic octopod	<i>Japetella diaphana</i>	0.4	<0.1	1	<0.1	1	1
Pacific glass shrimp	<i>Pasiphaea pacifica</i>	0.3	<0.1	143	2.2	19	13
jellyfish	<i>Cyanea</i> sp.	0.2	<0.1	1	<0.1	1	1
swordtail squid	<i>Chiroteuthis calyx</i>	0.2	<0.1	1	<0.1	-	-
popeye grenadier	<i>Coryphaenoides cinereus</i>	0.1	<0.1	1	<0.1	1	1
eulachon	<i>Thaleichthys pacificus</i>	<0.1	<0.1	1	<0.1	1	1
eelpout unid.	Zoarcidae (family)	<0.1	<0.1	17	0.3	2	2
Pacific viperfish	<i>Chauliodus macouni</i>	<0.1	<0.1	3	<0.1	2	2
blackmouth eelpout	<i>Lycodapus fierasfer</i>	<0.1	<0.1	9	0.1	9	9
salp unid.	Thaliacea (class)	<0.1	<0.1	27	0.4	-	-
brokenline lampfish	<i>Lampanyctus jordani</i>	<0.1	<0.1	1	<0.1	1	1
lanternfish	<i>Protomyctophum</i> sp.	<0.1	<0.1	6	<0.1	4	-
Hydromedusa (unid.)	Hydromedusa (unid.)	<0.1	<0.1	7	0.1	3	-
snailfish unid.	Liparidae (family)	<0.1	<0.1	17	0.3	3	-
opossum shrimp	<i>Mysidae</i> (family)	<0.1	<0.1	68	1.0	-	-
isopod unid.	Isopoda (order)	<0.1	<0.1	3	<0.1	-	-
helmet jelly	<i>Periphylla periphylla</i>	<0.1	<0.1	1	<0.1	1	1
fish larvae unid.	Actinopterygii (class)	<0.1	<0.1	6	<0.1	6	-
smelt unid.	Osmeridae (family)	<0.1	<0.1	1	<0.1	1	-
lanternfish unid.	Myctophidae (family)	<0.1	<0.1	3	<0.1	3	-
<b>Total</b>		<b>3,861.9</b>		<b>6,513</b>		<b>2,489</b>	<b>785</b>



Table 6. -- Numbers of walleye pollock measured and biological samples collected during the winter 2020 acoustic-trawl survey of Bogoslof.

Walleye Pollock									
Haul no.	Region Name	Gear type	Catch lengths	Weights	Maturities	Otoliths	Ovary weights	Ovaries preserved	Non-random collection
1	Bogoslof	LFS1421	9	9	9	9	6	2	-
2	Bogoslof	AWT	378	78	78	78	12	16	-
3	Bogoslof	LFS1421	398	80	80	80	10	13	-
4	Bogoslof	AWT	291	-	-	-	-	-	-
5	Bogoslof	LFS1421	127	80	80	80	36	1	-
6	Bogoslof	LFS1421	325	80	80	53	33	24	22
7	Bogoslof	AWT	231	-	-	-	-	-	-
8	Bogoslof	AWT	280	-	-	-	-	-	-
9	Bogoslof	LFS1421	235	60	60	55	46	8	20
10	Bogoslof	LFS1421	355	58	59	44	42	4	16
11	Bogoslof	AWT	274	-	-	-	-	-	-
12	Bogoslof	AWT	101	-	-	-	-	-	-
13	Bogoslof	LFS1421	274	40	40	40	35	-	20
14	Bogoslof	LFS1421	258	79	78	79	38	-	-
Total			3,536	564	564	518	258	68	78

Table 7. -- Walleye pollock biomass (tons (t)) estimated by survey area and management area from February-March acoustic-trawl surveys in the Bogoslof Island area between 1988 and 2020.

Year	<u>Bogoslof Survey Area</u>			<u>Central Bering Sea Specific Area</u>	
	Biomass (million t)	Area (nmi <sup>2</sup> )	Relative estimation error (%)	Biomass (million t)	Relative estimation error (%)
1988	2.396	--	--	2.396	--
1989	2.126	--	--	2.084	--
1990	--	No survey	--	--	--
1991	1.289	8,411	11.7	1.283	--
1992	0.940	8,794	20.4	0.888	--
1993	0.635	7,743	9.2	0.631	--
1994	0.490	6,412	11.6	0.490	--
1995	1.104	7,781	10.7	1.020	--
1996	0.682	7,898	19.6	0.582	--
1997	0.392	8,321	14.0	0.342	--
1998	0.492	8,796	19.0	0.432	19.0
1999	0.475	Conducted by Japan Fisheries Agency		0.393	--
2000	0.301	7,863	14.3	0.270	12.7
2001	0.232	5,573	10.2	0.208	11.8
2002	0.226	2,903	12.2	0.226	12.2
2003	0.198	2,993	21.5	0.198	21.5
2004	--	No survey	--	--	--
2005	0.253	3,112	16.7	0.253	16.7
2006	0.240	1,803	11.8	0.240	11.8
2007	0.292	1,871	11.5	0.292	11.5
2008	--	No survey	--	--	--
2009	0.110	1,803	19.2	0.110	19.2
2010	--	No survey	--	--	--
2011	--	No survey	--	--	--
2012	0.067	3,656	--	0.067	9.8*
2013	--	No survey	--	--	--
2014	0.112	1,150	11.8	0.112	11.8
2015	--	No survey	--	--	--
2016	0.508	1,400	11.0	0.508	11.0
2017	--	No survey	--	--	--
2018	0.663	1,500	42.5	0.663	42.5
2019	--	No survey	--	--	--
2020	0.353	1,449	15.8	0.353	15.8

\* The relative error for 2012 was computed for the primary survey area represented by transects 1-35 (1,455 nmi<sup>2</sup>)

Table 8. -- Numbers-at-length estimates (millions), and average fork length from February-March acoustic-trawl surveys of walleye pollock in the Bogoslof Island area. No surveys were conducted in 1990, 2004, 2008, 2010-2011, 2013, 2015, 2017, or 2019. The 1999 survey was conducted by the Japan Fisheries Agency. Lengths are in centimeters.

Length	1988	1989	1991	1992	1993	1994	1995	1996	1997	1998	1999	2000	2001	2002	2003	2005	2006	2007	2009	2012	2014	2016	2018	2020
10	0	0	0	0	0	0	<1	0	0	0	0	0	0	0	0	0	0	0	0	0	0	0	0	0
11	0	0	0	0	0	0	<1	0	0	0	0	0	0	0	0	0	0	0	0	0	0	0	0	0
12	0	0	0	0	0	0	1	0	0	0	0	0	0	0	0	0	0	0	0	0	0	0	0	0
13	0	0	0	0	0	0	<1	0	0	0	0	0	0	0	0	0	0	0	0	0	<1	0	0	0
14	0	0	0	0	0	0	<1	0	0	0	0	0	0	0	0	0	0	0	0	0	<1	0	0	0
15	0	0	0	0	0	0	0	0	0	0	0	0	0	0	0	0	0	0	0	0	0	0	0	0
16	0	0	0	0	0	0	0	0	0	0	0	0	0	0	0	0	0	0	0	0	0	0	0	0
17	0	0	0	0	0	0	0	0	0	0	0	0	0	0	0	0	0	0	0	0	0	0	0	0
18	0	0	0	0	0	0	0	0	0	0	0	0	0	0	0	0	0	0	0	0	0	0	0	0
19	0	0	0	0	0	0	0	0	0	0	0	0	0	0	0	0	0	0	0	0	0	0	0	0
20	0	0	0	0	0	0	0	0	0	0	0	0	0	0	0	0	0	0	0	0	0	0	0	0
21	0	0	0	0	0	0	0	0	0	0	0	0	0	0	0	0	0	0	0	0	0	0	0	0
22	0	0	<1	0	0	0	0	0	0	0	0	0	0	0	0	0	0	0	0	0	0	0	0	0
23	0	0	2	0	0	0	0	0	0	0	0	0	0	<1	0	0	0	0	0	0	0	0	0	0
24	0	0	1	0	0	0	0	0	0	0	0	0	0	0	0	0	0	0	0	0	0	0	0	0
25	0	0	0	0	0	0	0	0	0	0	0	0	0	0	0	0	0	0	0	0	0	0	0	0
26	0	0	<1	0	0	0	0	0	0	0	0	0	0	0	0	0	0	0	0	0	0	0	0	0
27	0	0	0	0	0	0	0	0	0	0	0	0	0	0	0	0	0	0	0	0	0	0	0	0
28	0	0	0	0	0	0	0	0	0	0	0	0	0	0	0	0	0	0	0	0	0	0	0	0
29	0	0	0	0	0	0	0	0	0	0	0	0	0	0	0	0	0	0	0	0	0	0	0	<1
30	0	0	0	0	0	0	0	0	0	0	0	0	0	<1	0	0	0	0	0	0	0	0	0	<1
31	0	0	0	<1	0	0	0	0	0	0	0	0	0	0	0	0	0	0	0	0	0	0	0	<1
32	0	0	0	<1	0	0	0	0	0	0	0	0	0	0	0	0	0	0	0	0	0	0	0	<1
33	0	0	0	<1	0	0	0	0	0	0	0	0	0	<1	<1	0	0	0	0	0	0	0	0	<1
34	0	0	0	0	0	0	<1	<1	0	<1	0	0	0	<1	<1	0	0	0	0	0	0	<1	0	<1
35	0	0	0	0	0	0	<1	0	<1	0	0	0	0	<1	0	0	0	0	0	0	0	<1	0	1
36	0	0	0	<1	0	0	<1	<1	<1	<1	0	0	0	1	0	0	0	0	0	0	0	6	0	1
37	9	3	<1	0	0	0	<1	<1	<1	<1	0	0	0	1	<1	<1	0	0	0	0	<1	12	1	2
38	6	0	2	<1	1	0	1	1	<1	1	0	0	<1	1	<1	1	<1	0	0	0	<1	27	0	2
39	16	4	5	0	2	<1	4	1	1	3	<1	<1	<1	2	<1	2	<1	<1	0	0	<1	42	1	2
40	24	3	7	1	4	3	12	4	1	7	1	<1	1	3	<1	7	2	0	0	0	2	33	4	1
41	27	4	19	3	5	6	20	8	2	9	6	1	1	4	<1	11	5	1	<1	<1	5	37	8	1

Table 8. – Continued.

Length	1988	1989	1991	1992	1993	1994	1995	1996	1997	1998	1999	2000	2001	2002	2003	2005	2006	2007	2009	2012	2014	2016	2018	2020
42	48	23	23	7	7	9	40	14	3	11	8	1	1	2	<1	12	10	2	<1	<1	8	43	9	1
43	118	33	31	14	6	14	40	17	4	11	13	3	1	5	1	11	16	4	<1	<1	9	56	30	1
44	179	54	36	18	7	21	41	21	5	10	13	3	2	5	2	11	20	8	<1	<1	8	61	38	1
45	329	159	46	28	8	21	50	23	7	9	17	4	3	7	3	13	23	11	<1	1	9	90	87	2
46	488	177	55	32	13	21	53	31	10	11	19	5	4	5	5	11	23	17	<1	2	7	74	79	3
47	547	389	79	42	22	18	40	36	14	9	14	6	5	9	5	11	18	17	1	2	7	98	143	5
48	476	434	130	68	28	17	55	36	15	12	11	6	5	7	7	10	17	20	1	2	6	88	108	11
49	389	431	168	102	46	16	47	37	18	15	10	5	6	6	6	8	14	14	2	2	5	60	158	23
50	248	366	205	129	69	39	52	40	21	20	16	6	6	5	7	8	9	18	2	3	7	59	94	28
51	162	279	189	144	76	46	58	45	24	23	11	8	6	5	4	9	9	15	5	3	2	26	57	32
52	80	168	160	118	73	52	78	52	26	28	20	10	7	4	4	7	7	13	5	2	2	19	59	36
53	48	85	122	106	73	49	81	52	26	35	17	13	8	6	4	7	5	12	6	2	4	8	41	47
54	19	50	63	67	66	43	88	53	31	41	21	16	9	7	3	7	5	10	8	2	2	7	27	43
55	12	13	40	41	50	37	81	48	28	38	33	21	13	9	5	8	3	9	8	2	2	3	9	25
56	4	5	17	27	29	26	69	40	24	35	38	20	13	12	7	6	6	8	8	2	3	3	5	26
57	3	8	8	13	14	17	58	37	22	30	33	24	16	13	7	7	5	6	6	3	4	3	5	18
58	1	1	4	6	9	10	47	28	17	27	36	23	14	14	10	6	7	7	6	3	4	1	<1	7
59	0	0	1	5	3	6	31	19	13	18	23	16	12	12	9	8	5	7	5	3	4	<1	0	5
60	0	0	1	1	1	3	17	12	12	13	15	13	12	12	13	7	7	6	2	4	3	2	1	7
61	2	0	1	<1	1	2	7	6	6	8	18	10	10	8	9	9	5	8	2	2	3	6	0	1
62	0	0	<1	<1	<1	1	4	2	3	5	13	7	6	6	7	7	5	7	1	2	2	1	0	2
63	0	0	0	0	0	<1	2	1	1	3	4	4	4	4	5	7	4	4	2	3	2	1	0	1
64	0	0	0	1	<1	0	1	<1	1	1	3	2	3	3	5	5	2	4	1	2	1	1	0	1
65	0	0	<1	0	0	0	<1	<1	<1	1	1	1	1	1	3	4	2	3	<1	<1	<1	0	0	<1
66	0	0	0	0	0	0	<1	0	<1	1	<1	<1	<1	1	1	2	2	3	<1	1	<1	0	0	1
67	0	0	0	0	0	0	0	0	0	0	1	<1	<1	<1	1	2	1	2	<1	1	<1	0	0	<1
68	0	0	0	0	0	0	1	0	0	<1	0	<1	<1	<1	<1	1	1	1	<1	<1	<1	0	0	0
69	0	0	0	0	0	0	0	0	0	0	0	0	<1	0	<1	<1	<1	1	<1	0	<1	1	0	<1
70	0	0	0	0	0	0	0	0	0	0	0	0	<1	<1	0	<1	<1	<1	<1	0	<1	0	0	0
71	0	0	0	0	0	0	0	0	0	0	0	0	0	0	0	<1	<1	<1	<1	0	0	0	0	0
72	0	0	0	0	0	0	0	0	0	0	0	0	0	0	0	<1	0	<1	<1	0	0	0	0	0
73	0	0	0	0	0	0	0	0	0	0	0	0	0	0	0	<1	0	0	<1	0	0	0	0	0
Total	3,236	2,687	1,419	975	613	478	1,081	666	337	435	416	229	170	181	134	225	239	236	73	49	113	868	964	338
Average length	47.2	48.7	49.6	50.6	51.4	51.0	50.9	51.4	52.8	52.5	53.4	55.0	55.1	53.1	55.7	51.2	49.7	52.3	55.3	55.5	49.6	45.7	48.2	52.5

Table 9. -- Biomass-at-length estimates (1,000 t) from February-March acoustic-trawl surveys of walleye pollock in the Bogoslof Island area. No surveys were conducted in 1990, 2004, 2008, 2010-2011, 2013, 2015, 2017, or 2019. The 1999 survey was conducted by the Japan Fisheries Agency. Lengths are in centimeters.

Length	1988	1989	1991	1992	1993	1994	1995	1996	1997	1998	1999	2000	2001	2002	2003	2005	2006	2007	2009	2012	2014	2016	2018	2020	
10	0	0	0	0	0	0	<1	0	0	0	0	0	0	0	0	0	0	0	0	0	0	0	0	0	
11	0	0	0	0	0	0	<1	0	0	0	0	0	0	0	0	0	0	0	0	0	0	0	0	0	
12	0	0	0	0	0	0	<1	0	0	0	0	0	0	0	0	0	0	0	0	0	0	0	0	0	
13	0	0	0	0	0	0	<1	0	0	0	0	0	0	0	0	0	0	0	0	0	<1	0	0	0	
14	0	0	0	0	0	0	<1	0	0	0	0	0	0	0	0	0	0	0	0	0	<1	0	0	0	
15	0	0	0	0	0	0	0	0	0	0	0	0	0	0	0	0	0	0	0	0	0	0	0	0	
16	0	0	0	0	0	0	0	0	0	0	0	0	0	0	0	0	0	0	0	0	0	0	0	0	
17	0	0	0	0	0	0	0	0	0	0	0	0	0	0	0	0	0	0	0	0	0	0	0	0	
18	0	0	0	0	0	0	0	0	0	0	0	0	0	0	0	0	0	0	0	0	0	0	0	0	
19	0	0	0	0	0	0	0	0	0	0	0	0	0	0	0	0	0	0	0	0	0	0	0	0	
20	0	0	0	0	0	0	0	0	0	0	0	0	0	0	0	0	0	0	0	0	0	0	0	0	
21	0	0	0	0	0	0	0	0	0	0	0	0	0	0	0	0	0	0	0	0	0	0	0	0	
22	0	0	<1	0	0	0	0	0	0	0	0	0	0	0	0	0	0	0	0	0	0	0	0	0	
23	0	0	<1	0	0	0	0	0	0	0	0	0	0	<1	0	0	0	0	0	0	0	0	0	0	
24	0	0	<1	0	0	0	0	0	0	0	0	0	0	0	0	0	0	0	0	0	0	0	0	0	
25	0	0	0	0	0	0	0	0	0	0	0	0	0	0	0	0	0	0	0	0	0	0	0	0	
26	0	0	<1	0	0	0	0	0	0	0	0	0	0	0	0	0	0	0	0	0	0	0	0	0	
27	0	0	0	0	0	0	0	0	0	0	0	0	0	0	0	0	0	0	0	0	0	0	0	0	
28	0	0	0	0	0	0	0	0	0	0	0	0	0	0	0	0	0	0	0	0	0	0	0	0	
29	0	0	0	0	0	0	0	0	0	0	0	0	0	0	0	0	0	0	0	0	0	0	0	<1	
30	0	0	0	0	0	0	0	0	0	0	0	0	0	6	0	0	0	0	0	0	0	0	0	0	<1
31	0	0	0	<1	0	0	0	0	0	0	0	0	0	0	0	0	0	0	0	0	0	0	0	<1	
32	0	0	0	<1	0	0	0	0	0	0	0	0	0	0	0	0	0	0	0	0	0	0	0	<1	
33	0	0	0	<1	0	0	0	0	0	0	0	0	0	<1	<1	0	0	0	0	0	0	0	0	<1	
34	0	0	0	0	0	0	<1	<1	0	<1	0	0	0	<1	<1	0	0	0	0	0	0	<1	0	<1	
35	0	0	0	0	0	0	<1	0	<1	0	0	0	0	<1	0	0	0	0	0	0	0	<1	0	<1	
36	0	0	0	<1	0	0	<1	<1	<1	<1	0	0	0	<1	0	0	0	0	0	0	0	2	0	<1	
37	3	1	<1	0	0	0	<1	<1	<1	<1	0	0	0	<1	<1	<1	0	0	0	0	<1	4	<1	1	
38	2	0	1	<1	<1	0	<1	<1	<1	<1	0	0	<1	1	<1	<1	<1	0	0	0	<1	11	0	1	
39	6	1	2	0	1	<1	2	1	1	1	<1	<1	<1	1	<1	1	<1	<1	0	0	<1	17	<1	1	
40	11	1	3	<1	2	1	6	2	1	3	1	<1	<1	2	<1	3	1	0	0	0	1	14	2	1	
41	13	2	8	1	2	3	10	4	1	4	6	1	<1	2	<1	5	2	<1	<1	<1	2	18	4	1	

Table 9. – Continued.

Length	1988	1989	1991	1992	1993	1994	1995	1996	1997	1998	1999	2000	2001	2002	2003	2005	2006	2007	2009	2012	2014	2016	2018	2020
42	24	11	11	3	4	5	21	7	1	6	7	1	<1	1	<1	6	5	1	<1	<1	4	21	4	1
43	64	17	16	7	3	8	22	9	2	6	12	2	1	3	<1	6	9	2	<1	<1	5	28	15	1
44	105	30	20	10	4	13	25	13	3	6	12	2	2	4	1	6	12	5	<1	<1	5	32	21	<1
45	207	94	28	16	5	14	33	15	5	6	16	3	2	5	2	8	15	7	<1	1	6	49	51	1
46	329	113	36	21	9	15	37	22	7	8	18	3	3	4	4	8	17	12	<1	1	5	43	48	3
47	395	268	57	29	17	14	30	26	11	7	14	5	4	7	4	9	14	13	1	1	5	59	90	4
48	367	323	101	52	22	14	45	29	12	10	11	5	4	6	6	8	15	17	1	2	5	56	72	9
49	321	346	141	84	40	14	40	32	16	13	11	5	5	6	6	7	13	13	2	2	4	40	109	19
50	218	315	187	116	64	36	48	36	20	19	18	5	6	5	7	7	9	18	2	3	6	42	72	24
51	152	258	186	140	76	46	57	43	24	23	12	8	6	5	4	9	10	16	5	3	2	19	46	30
52	80	166	171	124	78	56	82	54	29	29	23	11	8	4	5	8	7	15	6	2	2	15	48	35
53	51	90	140	120	83	55	90	57	30	39	20	15	9	6	5	8	6	15	8	3	4	7	35	49
54	21	57	78	82	79	52	104	62	38	49	25	19	11	8	4	9	6	13	11	2	2	6	26	47
55	14	16	53	53	64	48	102	59	36	47	39	27	17	12	6	11	5	13	13	2	3	3	8	30
56	6	6	24	39	40	35	92	53	33	48	47	27	17	16	11	9	10	13	12	2	5	3	6	33
57	4	11	12	20	21	24	82	52	32	43	41	35	24	19	11	10	7	10	9	4	6	3	5	24
58	1	1	7	9	14	16	71	41	26	41	45	34	22	22	16	10	11	11	10	5	7	1	<1	10
59	0	0	1	8	4	10	49	29	21	28	28	26	20	19	15	14	9	10	9	5	7	<1	0	7
60	0	0	3	3	2	5	28	20	21	22	18	22	20	21	23	13	11	13	5	6	4	2	1	13
61	3	0	2	1	2	4	12	11	11	14	23	19	18	15	17	17	8	14	5	4	5	7	0	2
62	0	0	1	1	<1	2	8	4	6	10	15	13	12	12	15	13	10	15	2	4	4	1	0	3
63	0	0	0	0	0	<1	4	3	3	6	5	7	8	8	11	14	8	9	4	6	4	1	0	2
64	0	0	0	1	<1	0	1	1	1	2	3	4	6	6	11	10	6	9	2	4	3	1	0	2
65	0	0	1	0	0	0	<1	1	1	1	2	2	3	2	7	9	4	7	1	<1	2	0	0	<1
66	0	0	0	0	0	0	<1	0	<1	1	<1	1	1	2	4	5	5	6	1	2	2	0	0	3
67	0	0	0	0	0	0	0	0	0	0	1	1	<1	1	2	5	3	5	<1	2	1	0	0	<1
68	0	0	0	0	0	0	3	0	0	<1	0	<1	<1	1	1	2	2	3	<1	<1	<1	0	0	0
69	0	0	0	0	0	0	0	0	0	0	0	0	<1	0	<1	1	1	3	<1	0	<1	1	0	<1
70	0	0	0	0	0	0	0	0	0	0	0	0	<1	<1	0	<1	<1	1	<1	0	<1	0	0	0
71	0	0	0	0	0	0	0	0	0	0	0	0	0	0	0	<1	<1	1	0	0	0	0	0	0
72	0	0	0	0	0	0	0	0	0	0	0	0	0	0	0	<1	0	<1	0	0	0	0	0	0
73	0	0	0	0	0	0	0	0	0	0	0	0	0	0	0	<1	0	0	0	0	0	0	0	0
Total	2,396	2,126	1,289	940	635	490	1,104	682	392	492	475	301	232	226	198	253	240	292	110	67	112	508	663	353

Table 10. -- Numbers-at-age estimates (millions) from February-March acoustic-trawl surveys of walleye pollock in the Bogoslof Island area. No surveys were conducted in 1990, 2004, 2008, 2010-2011, 2013, 2015, 2017, or 2019. The 1999 survey was conducted by the Japan Fisheries Agency. Ages are in years.

Age	1988	1989	1990	1991	1992	1993	1994	1995	1996	1997	1998	1999	2000	2001	2002	2003	2004	2005	2006	2007	2008	2009	2010	2011	2012	2013	2014	2015	2016	2017	2018	2019	2020	
0	--	--	--	--	--	--	--	--	--	--	--	--	--	--	--	--	--	--	--	--	--	--	--	--	--	--	--	--	--	--	--	--	--	
1	--	--	--	--	--	--	--	1	--	--	--	--	--	--	--	--	--	--	--	--	--	--	--	--	--	--	<1	--	--	--	--	--	--	
2	--	--	--	4	--	--	--	--	--	--	--	--	--	--	<1	--	--	--	--	--	--	--	--	--	--	--	--	--	--	--	--	--	<1	
3	--	--	--	--	1	1	--	2	--	--	--	--	--	--	9	<1	--	--	--	--	--	--	--	--	--	--	<1	--	3	--	--	--	10	
4	--	6	--	2	2	33	21	6	<1	<1	<1	2	1	1	5	8	--	5	4	1	--	--	--	<1	--	1	--	170	--	--	--	3		
5	28	15	--	12	27	17	86	75	6	4	11	5	6	14	3	6	--	81	55	8	--	1	--	--	1	--	34	--	41	--	59	--	<1	
6	327	58	--	46	54	44	26	278	96	16	61	29	4	12	41	7	--	31	104	92	--	1	--	--	15	--	31	--	161	--	152	--	4	
7	247	363	--	213	97	46	38	105	187	55	34	77	14	10	11	25	--	13	18	70	--	7	--	--	10	--	11	--	367	--	81	--	14	
8	164	147	--	93	74	48	36	68	85	88	70	34	30	10	8	11	--	11	6	17	--	23	--	--	2	--	14	--	99	--	381	--	27	
9	350	194	--	160	71	42	36	80	40	38	77	50	16	14	6	4	--	22	6	3	--	26	--	--	1	--	7	--	17	--	247	--	56	
10	1,201	91	--	44	55	28	17	53	37	28	32	75	28	12	7	5	--	7	9	3	--	8	--	--	2	--	3	--	9	--	27	--	107	
11	288	1,105	--	92	57	51	27	54	24	16	25	29	45	18	8	4	--	3	3	8	--	1	--	--	7	--	<1	--	--	--	14	--	89	
12	287	222	--	60	33	25	23	19	24	16	21	27	21	31	14	10	--	5	2	4	--	1	--	--	8	--	1	--	1	--	3	--	21	
13	202	223	--	373	34	27	13	59	12	13	19	25	16	13	30	8	--	4	4	1	--	1	--	--	1	--	5	--	--	--	--	--	5	
14	89	82	--	119	142	42	9	32	36	7	18	16	11	7	9	26	--	5	5	5	--	<1	--	--	<1	--	4	--	--	--	--	--	<1	
15	27	90	--	41	164	92	45	12	18	13	9	12	11	9	7	6	--	11	8	5	--	<1	--	--	<1	--	2	--	--	--	--	--	--	
16	17	30	--	38	59	47	36	31	4	5	15	10	9	8	9	5	--	12	5	3	--	1	--	--	<1	--	0	--	--	--	--	--	--	
17	7	60	--	29	8	25	28	103	16	4	5	8	3	5	5	3	--	6	7	6	--	1	--	--	<1	--	<1	--	--	--	--	--	--	
18	3	--	--	32	15	11	16	60	35	12	8	6	6	1	4	5	--	4	2	4	--	<1	--	--	<1	--	<1	--	--	--	--	--	--	
19	--	--	--	56	22	11	4	18	26	12	10	3	3	3	2	1	--	3	1	3	--	1	--	--	<1	--	--	--	--	--	--	--	--	
20	--	--	--	4	42	11	4	5	12	7	15	4	2	1	2	<1	--	1	2	1	--	<1	--	--	--	--	--	--	--	--	--	--	--	
21	--	--	--	2	13	10	8	5	3	2	4	3	1	--	--	1	--	<1	<1	<1	--	<1	--	--	--	--	--	--	--	--	--	--	--	
22	--	--	--	--	3	1	2	6	2	1	1	2	1	--	--	--	--	--	--	1	--	--	--	--	--	--	--	--	--	--	--	--	--	
23	--	--	--	--	1	1	2	6	1	<1	--	<1	--	<1	<1	--	--	--	--	--	--	--	--	--	--	--	--	--	--	--	--	--	--	--
24	--	--	--	--	--	--	1	2	--	1	--	--	<1	<1	<1	--	--	<1	--	1	--	--	--	--	--	--	--	--	--	--	--	--	--	--
25	--	--	--	--	--	--	--	--	--	--	--	--	--	--	<1	--	--	--	--	--	--	--	--	--	--	--	--	--	--	--	--	--	--	--
Total	3,236	2,687	--	1,419	975	613	478	1,081	666	336	435	416	229	170	181	134	--	225	239	236	--	73	--	--	49	--	113	--	868	--	964	--	338	

Table 11. -- Biomass-at-age estimates (1,000 t) from February-March acoustic-trawl surveys of walleye pollock in the Bogoslof Island area. No surveys were conducted in 1990, 2004, 2008, 2010-2011, 2013, 2015, 2017 or 2019. The 1999 survey was conducted by the Japan Fisheries Agency. Ages are in years.

Age	1988	1989	1990	1991	1992	1993	1994	1995	1996	1997	1998	1999	2000	2001	2002	2003	2004	2005	2006	2007	2008	2009	2010	2011	2012	2013	2014	2015	2016	2017	2018	2019	2020	
0	--	--	--	--	--	--	--	--	--	--	--	--	--	--	--	--	--	--	--	--	--	--	--	--	--	--	--	--	--	--	--	--	--	--
1	--	--	--	--	--	--	--	<1	--	--	--	--	--	--	--	--	--	--	--	--	--	--	--	--	--	<1	--	--	--	--	--	--	--	--
2	--	--	--	<1	--	--	--	--	--	--	--	--	--	--	<1	--	--	--	--	--	--	--	--	--	--	--	--	--	--	--	--	--	--	<1
3	--	--	--	--	<1	<1	--	1	--	--	--	--	--	--	5	<1	--	--	--	--	--	--	--	--	--	<1	--	1	--	--	--	--	4	
4	--	2	--	1	1	19	13	3	<1	<1	<1	2	<1	<1	3	7	--	3	2	1	--	0	--	--	<1	--	1	--	76	--	--	--	2	
5	15	7	--	6	21	12	60	49	4	2	7	6	4	12	2	5	--	52	36	6	--	1	--	--	1	--	19	--	20	--	31	--	<1	
6	192	41	--	25	38	39	22	208	69	11	38	28	3	11	34	6	--	25	85	80	--	1	--	--	15	--	23	--	92	--	93	--	3	
7	156	241	--	143	67	43	40	83	165	50	30	78	12	10	10	26	--	14	19	86	--	9	--	--	11	--	10	--	228	--	56	--	12	
8	115	111	--	75	59	47	39	72	76	95	74	37	30	12	9	12	--	15	7	25	--	33	--	--	3	--	19	--	66	--	264	--	27	
9	251	149	--	149	67	44	40	96	46	44	94	60	18	18	8	6	--	29	8	4	--	39	--	--	1	--	12	--	13	--	185	--	58	
10	910	68	--	44	57	31	21	64	45	38	40	90	40	16	9	8	--	10	15	6	--	13	--	--	4	--	5	--	11	--	20	--	117	
11	226	895	--	94	61	59	32	71	31	23	36	35	63	26	12	7	--	6	4	14	--	2	--	--	12	--	<1	--	--	--	11	--	98	
12	233	187	--	59	36	27	28	26	33	22	29	33	32	50	23	18	--	9	3	7	--	2	--	--	14	--	1	--	1	--	3	--	24	
13	167	194	--	378	37	30	17	77	17	18	27	30	25	20	48	14	--	8	6	1	--	2	--	--	2	--	10	--	--	--	--	--	7	
14	82	72	--	116	150	47	11	42	49	11	26	19	18	11	15	47	--	10	9	11	--	1	--	--	<1	--	8	--	--	--	--	--	1	
15	23	81	--	39	169	107	53	17	24	20	13	14	16	14	12	11	--	21	15	12	--	1	--	--	1	--	3	--	--	--	--	--	--	
16	16	24	--	38	63	54	43	38	6	7	22	13	15	14	15	8	--	25	9	6	--	2	--	--	<1	--	<1	--	--	--	--	--	--	
17	7	52	--	31	9	28	32	131	21	5	8	10	6	7	8	5	--	11	13	12	--	2	--	--	1	--	<1	--	--	--	--	--	--	
18	3	--	--	32	15	11	18	74	43	17	10	7	8	2	6	10	--	8	3	8	--	1	--	--	<1	--	1	--	--	--	--	--	--	
19	--	--	--	55	23	14	5	22	32	17	13	3	5	5	3	2	--	5	2	6	--	1	--	--	<1	--	--	--	--	--	--	--	--	
20	--	--	--	4	44	12	5	6	14	9	19	4	3	2	3	1	--	1	3	2	--	<1	--	--	--	--	--	--	--	--	--	--	--	
21	--	--	--	1	15	10	9	5	4	2	5	4	2	--	--	2	--	<1	1	1	--	<1	--	--	--	--	--	--	--	--	--	--	--	
22	--	--	--	--	3	1	2	8	2	1	1	3	2	--	--	--	--	--	--	2	--	--	--	--	--	--	--	--	--	--	--	--	--	
23	--	--	--	--	1	1	2	7	1	<1	--	1	--	<1	<1	--	--	--	--	--	--	--	--	--	--	--	--	--	--	--	--	--	--	--
24	--	--	--	--	--	--	1	3	--	1	--	--	1	<1	1	--	--	<1	--	1	--	--	--	--	--	--	--	--	--	--	--	--	--	--
25	--	--	--	--	--	--	--	--	--	--	--	--	--	--	<1	--	--	--	--	--	--	--	--	--	--	--	--	--	--	--	--	--	--	--
Total	2,396	2,126	--	1,289	940	635	490	1,104	682	392	492	475	301	232	226	198	--	253	240	292	--	110	--	--	67	--	112	--	508	--	663	--	353	



Table 12. -- Effect of changing post-processing parameters on estimated walleye pollock abundance and biomass observed during the winter 2020 acoustic-trawl survey in the Bogoslof Island area. The primary analysis (A-1) applied the nearest-haul approach, allocated backscatter to all species caught in the nearest haul, net-selectivity corrections were implemented, but no equal-sex correction was made. In contrast, the historical analyses pooled pollock lengths by area, allocated backscatter only to pollock, equal-sex correction was applied, but no net selectivity corrections were implemented.

Alternative Analysis		% Change relative to the 2020 primary analysis (A-1)	
		Abundance	Biomass
A-2	Pooled pollock lengths, pollock only, equal-sex, no net-selectivity	7.25	1.40
A-3	Nearest-haul, all species, equal-sex, no net-selectivity	4.80	-1.36
A-8	Pooled pollock lengths, pollock only, no equal-sex, no net-selectivity	3.32	3.44
A-9	Nearest-haul, all species, no equal-sex, no net-selectivity	1.24	1.04
A-12	Pooled pollock lengths, pollock only, no equal-sex, with net-selectivity for pollock	3.32	3.44

Table 13. -- Unweighted percent female walleye pollock in spawning and post-spawning maturity condition by regions during Bogoslof survey years 1988-2020. Percentages greater than 50% are outlined, and n = total number of female pollock examined.

Year	Date	% Pollock females spawning and post-spawning by region*					
		Samalga		Umnak		Unalaska	
		%	n	%	n	%	n
1988	12-26 Feb	26.8	183	20.0	744	10.7	326
	27 Feb - 1 Mar	56.7	1440				
	2-3 Mar	60.4	48	71.7	530		
1989	6-7 Feb	0.5	200	0.0	50		
	23-25 Feb	29.4	51	7.3	55		
	1-7 Mar	86.5	133	88.7	97	10.0	50
1991	24-27 Feb	9.2	163	7.5	212		
	1-3 Mar	36.4	118	20.9	67		
	8-10 Mar	59.1	127	71.2	59		
	15 Mar					97.7	44
1992	29 Feb - 8 Mar	1.0	101	0.8	491	2.4	41
1993	27 Feb - 5 Mar	5.0	160	2.6	470	0.0	98
	12 Mar			67.0	97		
1994	27 Feb - 9 Mar	14.7	170	6.3	816	0.0	64
1995	26 Feb - 4 Mar	24.4	127	12.1	141	12.0	117
	5-8 Mar	6.5	169	24.5	94		
1996	27 Feb - 8 Mar	3.0	368	1.8	220	0.0	100
1997	1-8 Mar	14.7	224	4.0	125	4.3	69
	9-10 Mar	30.0	30	37.0	100	18.2	99
1998	2-9 Mar	4.8	294	13.6	199	2.4	85
2000	2-12 Mar	0.9	218	1.7	118	4.2	24
2001	5-11 Mar	2.3	350	0.9	110		
2002	5-8 Mar	2.0	358	23.0	148		
2003	9-13 Mar	8.7	69	15.3	111		
2005	7-13 Mar	3.6	225	39.0	349		
2006	4-9 Mar	6.7	357	59.8	214		
2007	1-10 Mar	21.4	313	26.5	215		
2009	7-13 Mar	0.8	119	4.8	105		
2012	7-15 Mar	5.2	115	9.6	94		
2014	7-11 Mar	7.7	91	60.5	76		
2016	4-8 Mar	83.9	285	71.4	273		
2018	3-7 Mar			81.6	223		
2020	19-23 Feb	1.2	169	13.4	232		

\*Regions defined:

Samalga: west of 168° 30' W, and south of 55° N.

Umnak: between 168° 30' W and 167° W, and south of 55° N.

Unalaska: between 167° W and 166° W, and south of 55° N.

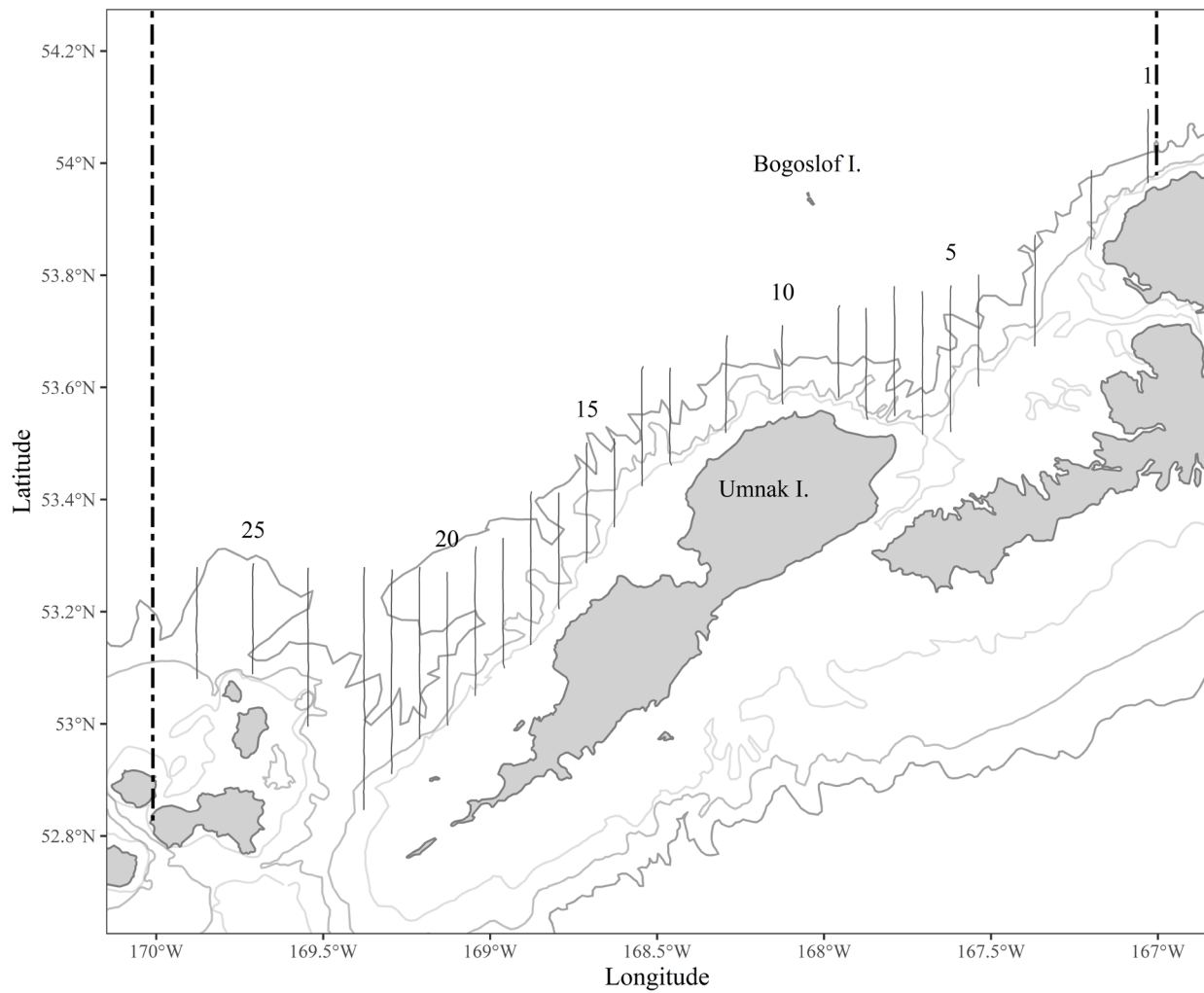


Figure 1. -- Transect coverage during the winter 2020 acoustic-trawl survey of the Bogoslof Island region. Transect numbers are labeled, and the Central Bering Sea Specific area is bounded by dashed lines.

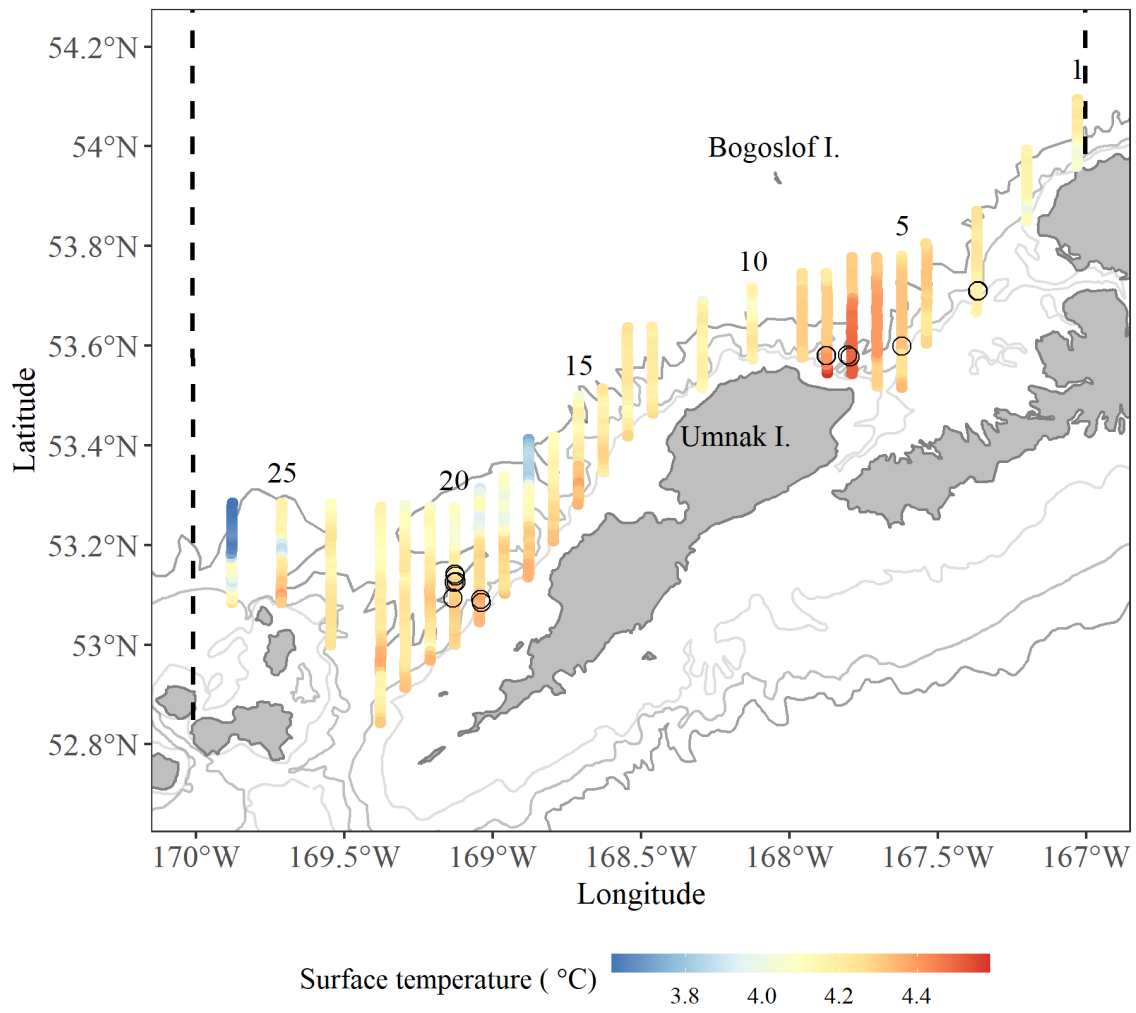


Figure 2. -- Surface water temperatures (°C) recorded at 5-second intervals during the winter 2020 acoustic-trawl survey of the Bogoslof Island region. Transect numbers are labeled, trawl haul locations are indicated by circles, and the Central Bering Sea Specific area is bounded by dashed lines.

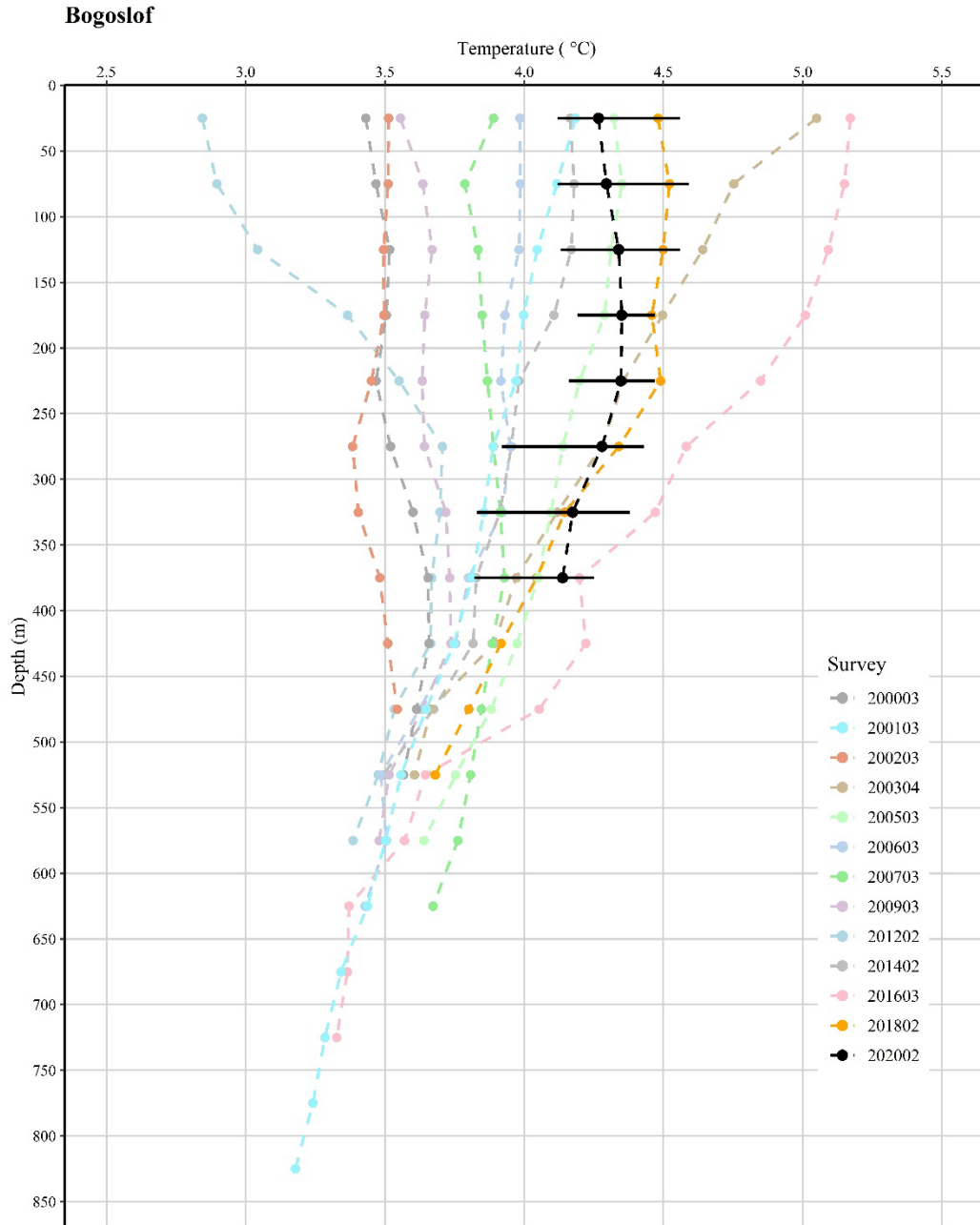


Figure 3. -- Average temperature (°C) by 50-m depth intervals observed during hauls from the winter 2000-2003, 2005-2007, 2009, 2012, 2014, 2016, 2018, and 2020 acoustic-trawl surveys of walleye pollock in the Bogoslof Island area. The horizontal bars represent temperature ranges observed during the 2020 survey. Note: Temperature data from the 2003 survey were collected from only three locations and temperature data from the 2018 survey were collected from only five locations.

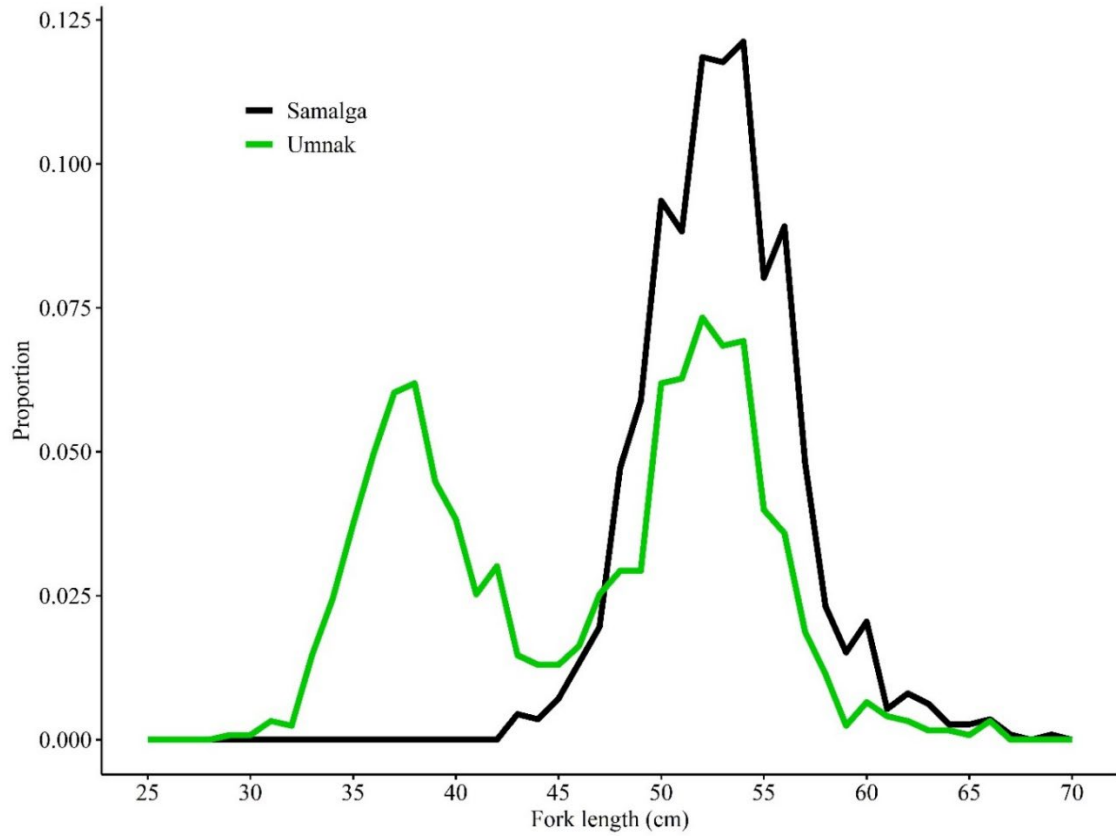


Figure 4. -- Proportion at length for walleye pollock measured in the Umnak and Samalga regions during the 2020 acoustic-trawl survey of walleye pollock in the Bogoslof Island area.

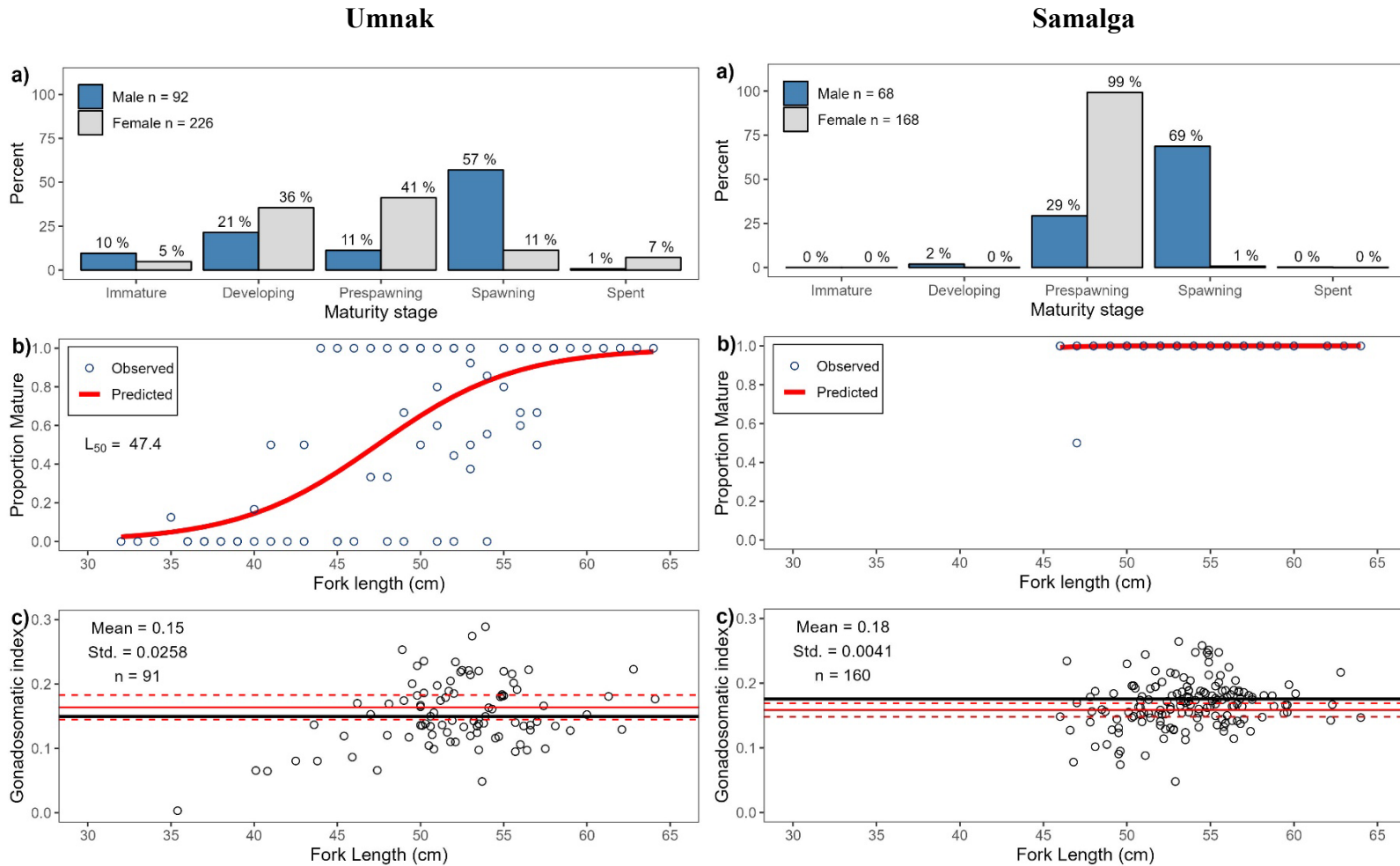


Figure 5. -- Walleye pollock (> 30 cm, random) maturity in the Umnak and Samalga regions. a) Pollock maturity stages by sex, with percentages annotated for each sex and maturity stage (random fish), b) proportion mature (i.e., pre-spawning, spawning, or spent by 1-cm size group for female pollock, c) gonadosomatic index (GSI) for pre-spawning female pollock as a function of fork length, with the mean GSI indicated by the solid black line. The historical GSI (2003-2018) mean and standard deviation ( $\pm 1$  std. dev.) are depicted by the solid red line and dashed red lines, respectively. All maturity quantities were weighted by local pollock abundance.

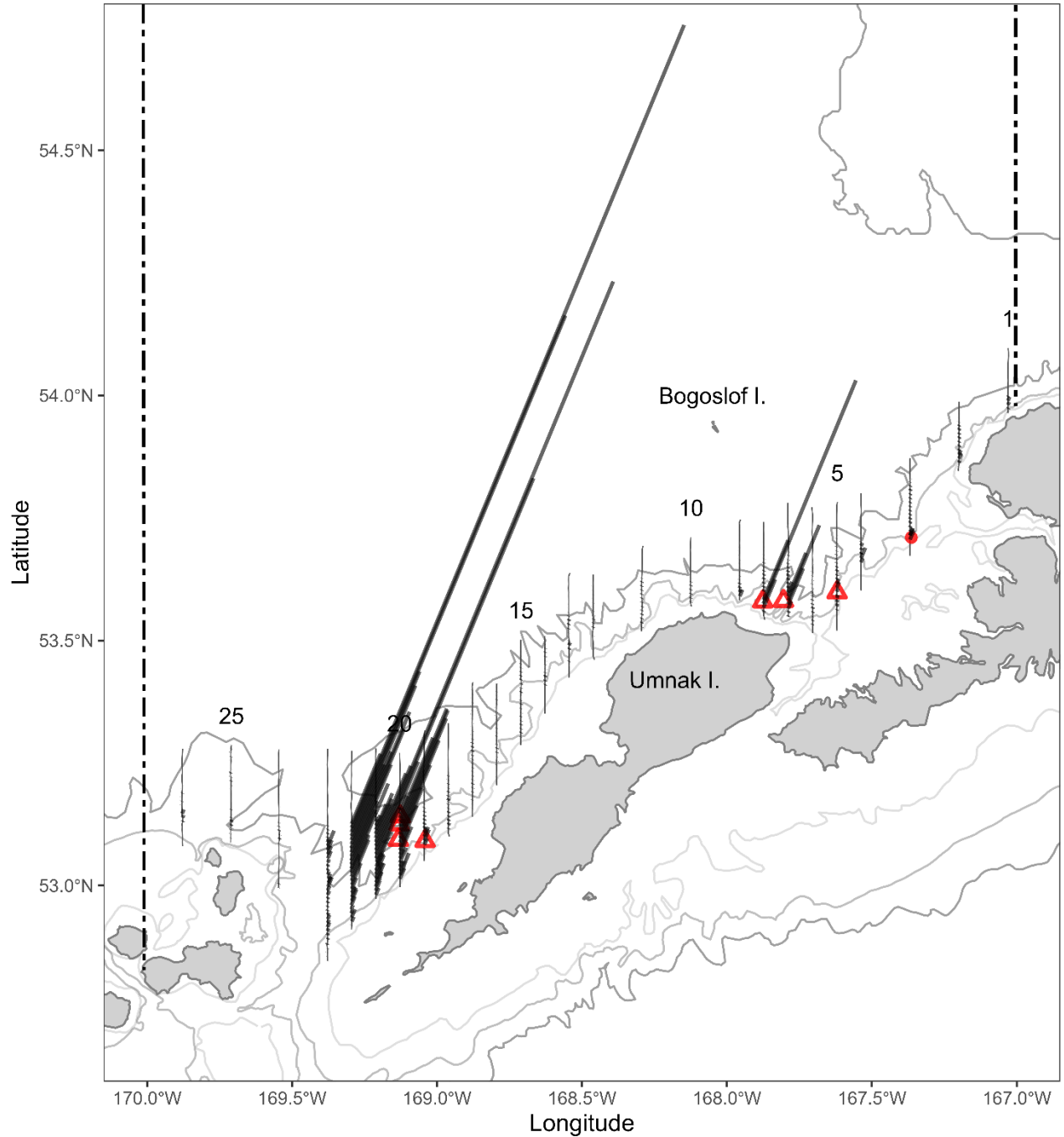


Figure 6. -- Transects, haul locations, and walleye pollock biomass per unit area ( $t/nmi^2$ ) observed along transects during the winter 2020 acoustic-trawl survey of walleye pollock in the southeast Aleutian Basin near Bogoslof Island. Trawl haul locations are indicated by red circles (AWT) and red triangles (LFS1421), and the Central Bering Sea Specific area is indicated between the two dash-dotted lines. The Umnak stratum includes transects 1-10, and the Samalga stratum includes transects 11-26. The maximum visible bar height represents 31,321 ( $t/nmi^2$ ).



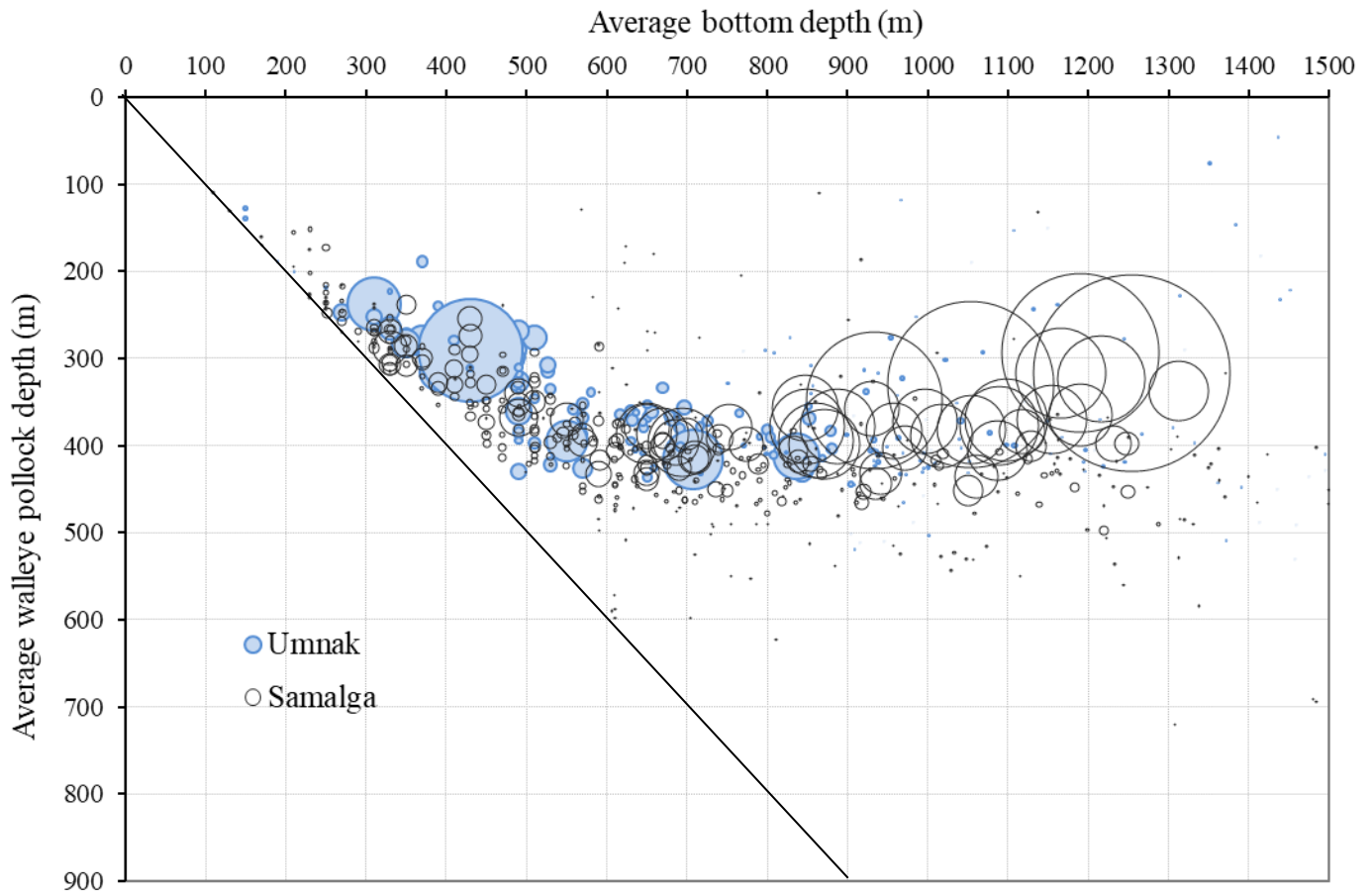


Figure 7. -- Average walleye pollock depth (weighted by biomass) versus bottom depth (m), per 0.5 nmi sailed distance for the Umnak and Samalga regions during the winter 2020 acoustic-trawl survey of walleye pollock in the Bogoslof Island area. The maximum bubble size for a 0.5 nmi interval was 46,980 t in the Samalga region. The diagonal line indicates where the average pollock depth equals bottom depth. Note that bottom depth measurements were limited to 1,500 m.

**Bogoslof total abundance:  
337.8 million fish and 353.1 thousand metric tons**

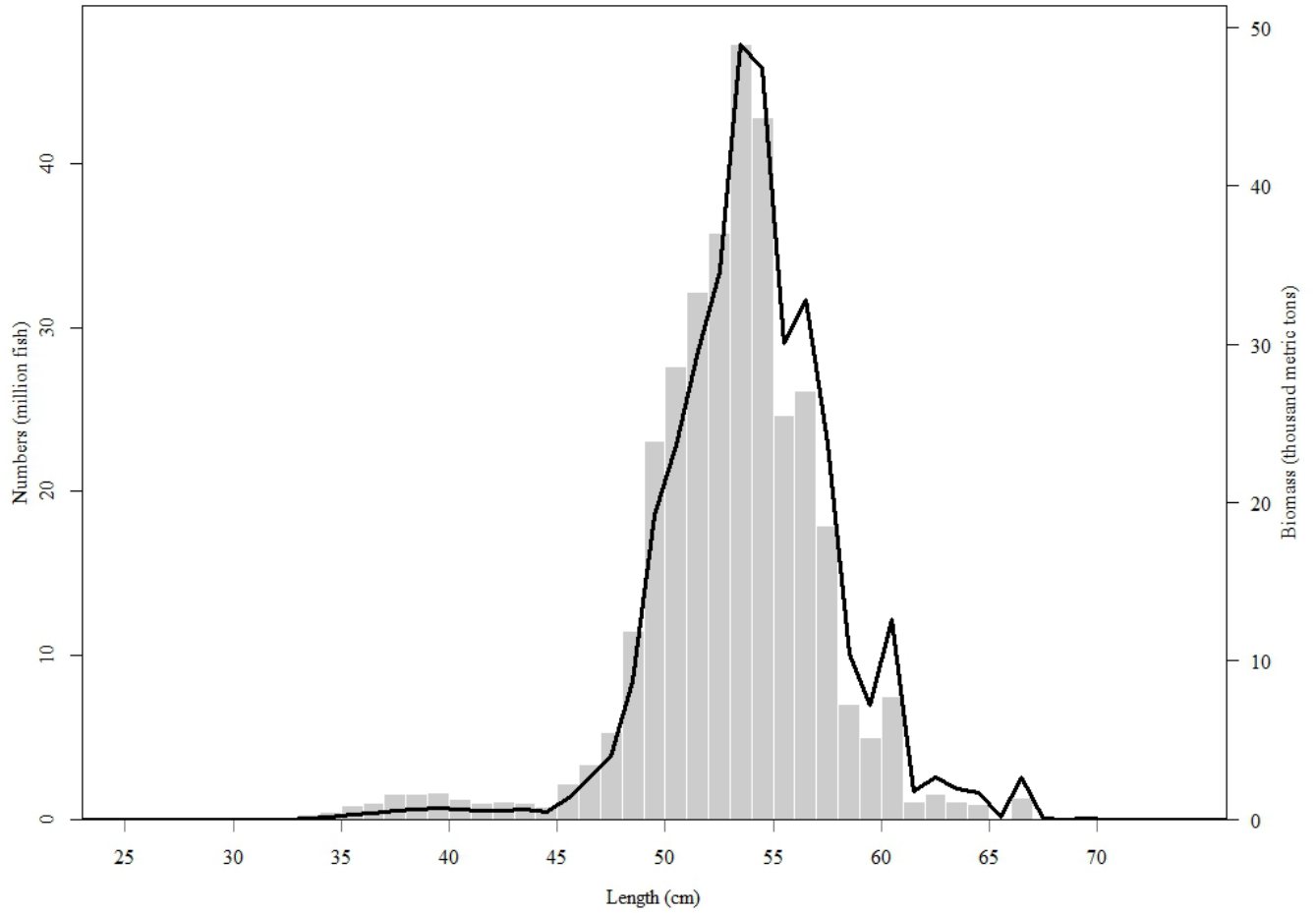


Figure 8. -- Numbers-at-length and biomass-at-length estimates from the winter 2020 acoustic-trawl survey of walleye pollock in the Bogoslof Island area.

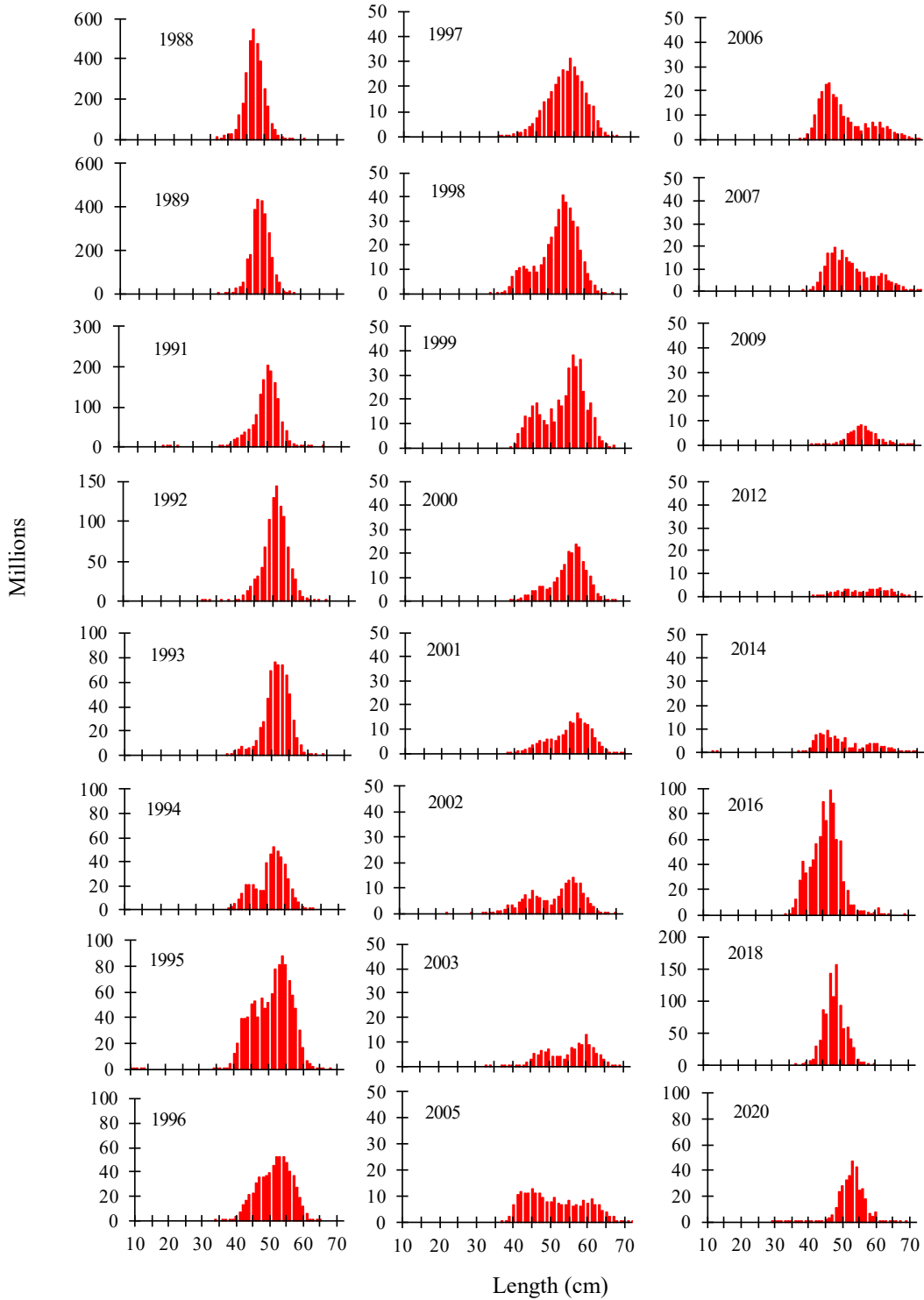


Figure 9. -- Numbers-at-length estimates (millions) from winter acoustic-trawl surveys of spawning pollock near Bogoslof Island. No surveys were conducted in 1990, 2004, 2008, 2010-2011, 2013, 2015, 2017, or 2019. The 1999 survey was conducted by Japan. Note: Y-axis scales differ.

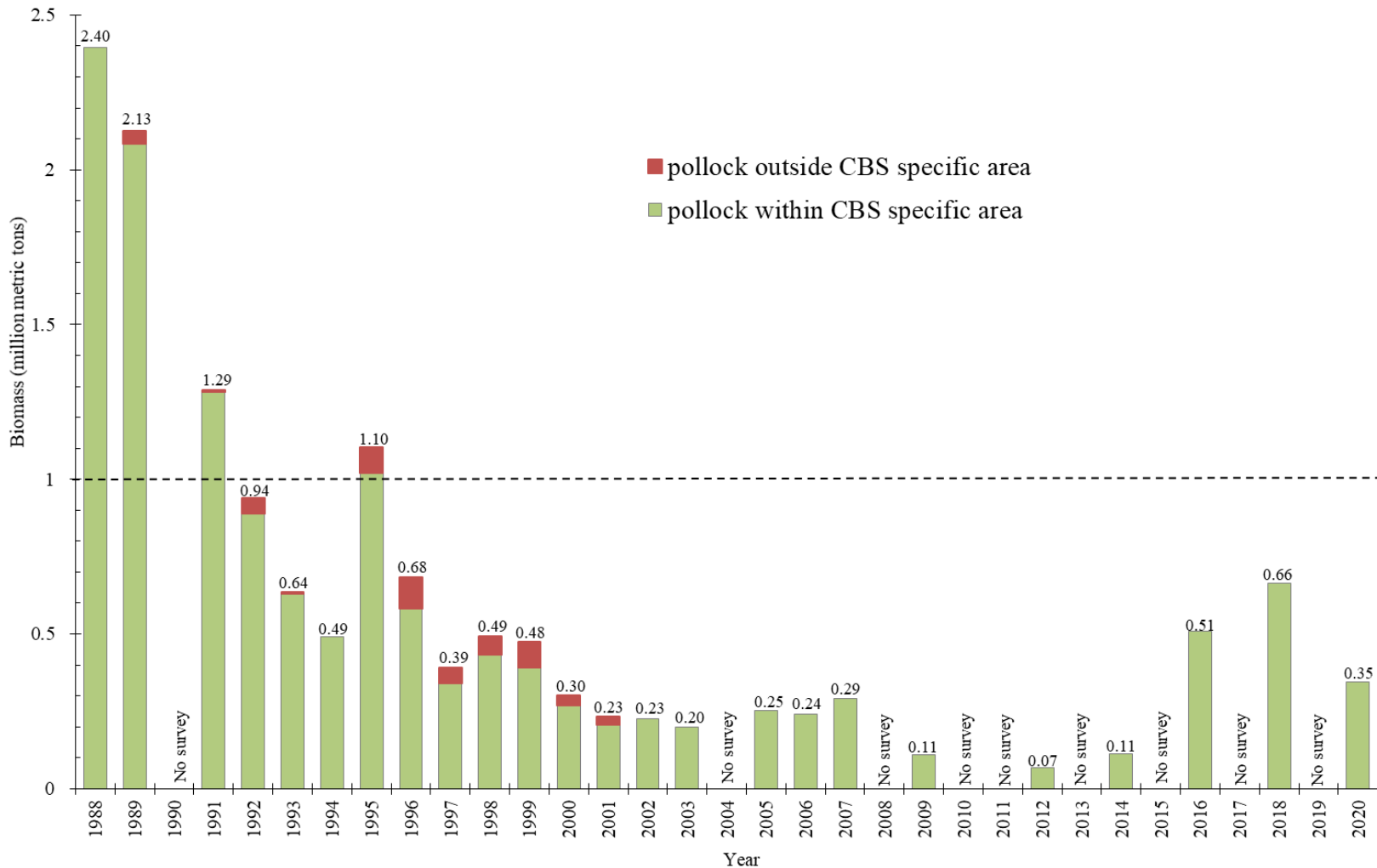


Figure 10. -- Biomass estimates for the winter acoustic-trawl surveys for walleye pollock in the Bogoslof Island area, within and outside the Central Bering Sea (CBS) specific area, 1988-2020. The United States conducted all but the 1999 survey, which was conducted by Japan. There were no surveys in 1990, 2004, 2008, 2010-2011, 2013, 2015, 2017 or 2019. Total pollock biomass (million metric tons) for each survey year is indicated on top of each bar. Pollock within the CBS specific area must reach 1 million metric tons before targeted pollock fishing can reconsidered in the Aleutian Basin.

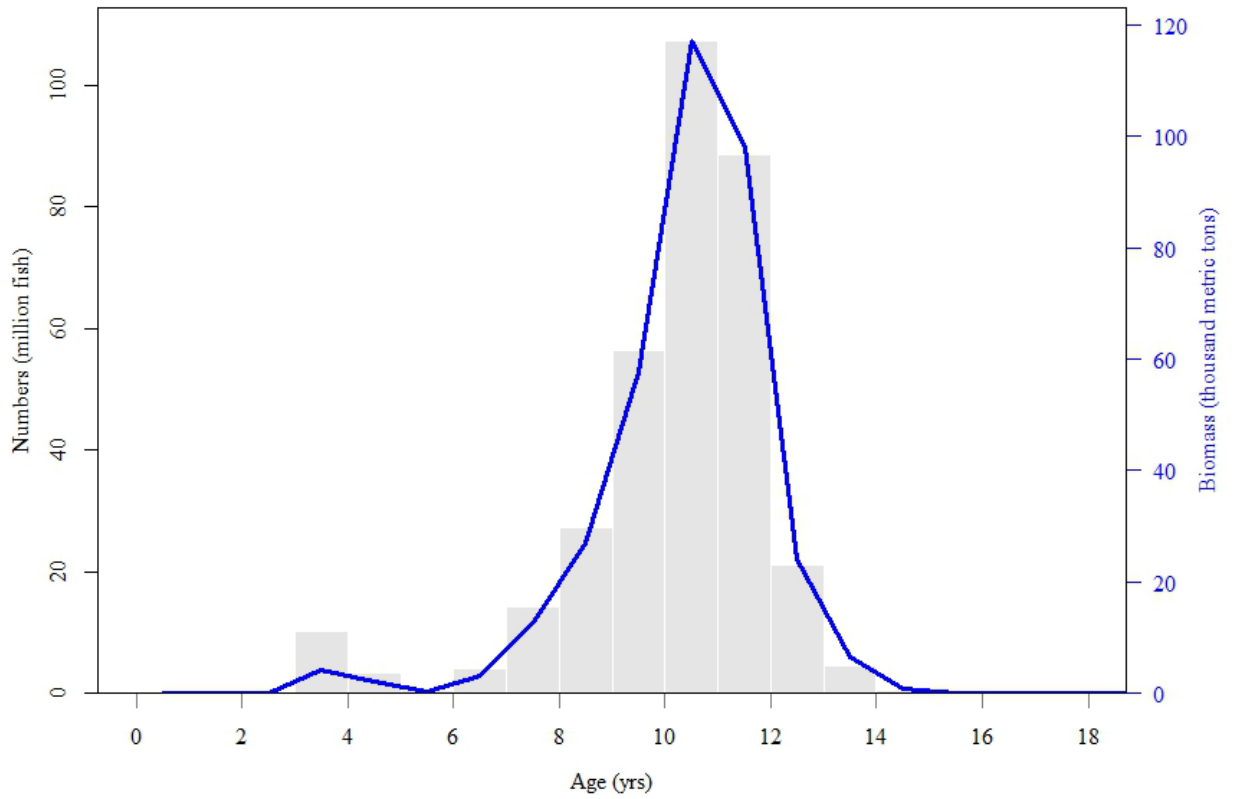


Figure 11. -- Numbers-at-age (grey bars; millions and biomass-at-age (blue line; thousand metric tons) estimates from the winter 2020 acoustic-trawl survey of walleye pollock in the Bogoslof Island area.

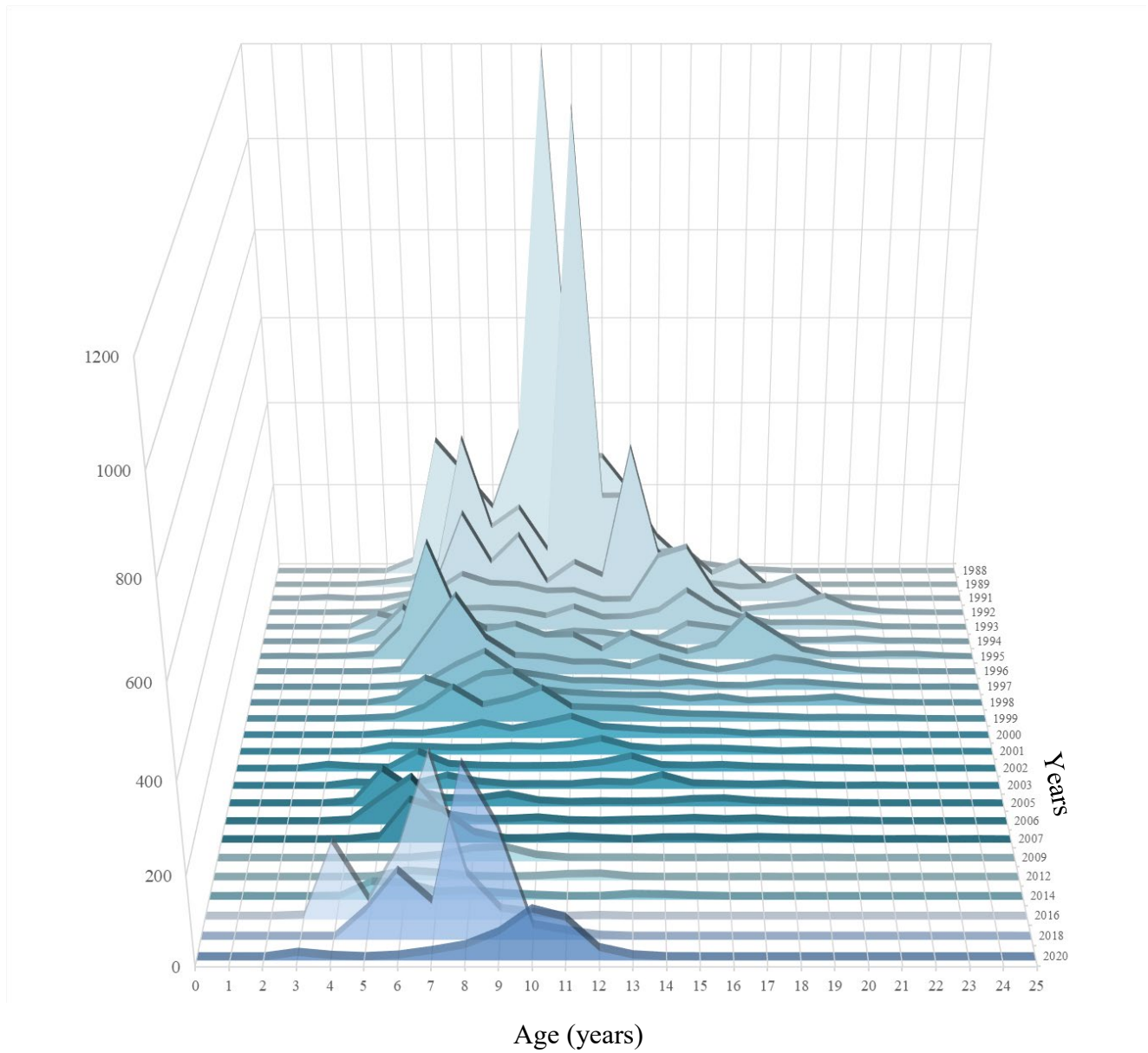


Figure 12. -- Numbers-at-age estimates (millions) from acoustic-trawl surveys of pollock near Bogoslof Island. No surveys were conducted in 1990, 2004, 2008, 2010-2011, 2013, 2015, 2017, or 2019.

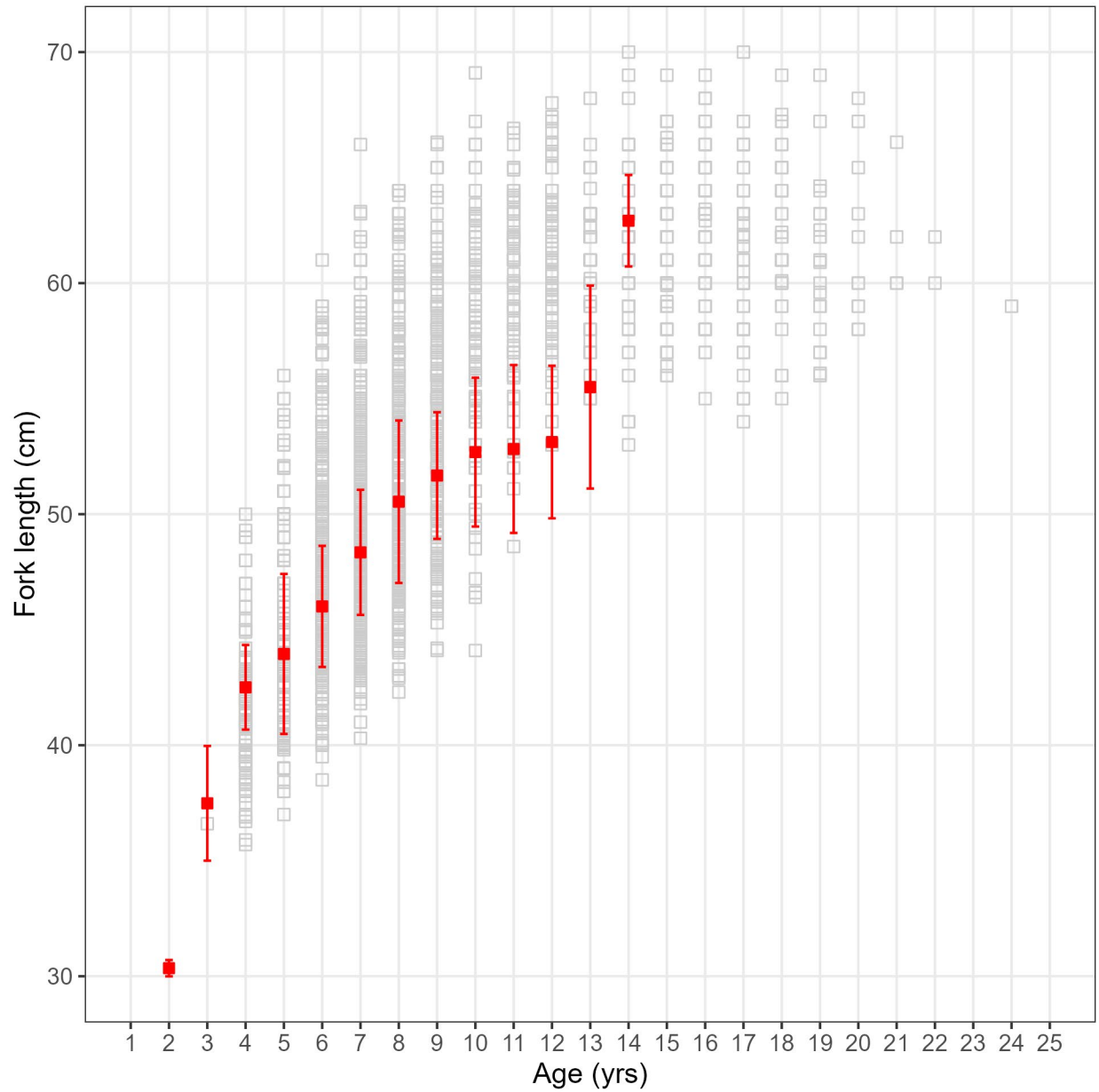


Figure 13. -- Walleye pollock average length-at-age from historic winter Bogoslof acoustic-trawl surveys (2003-present; grey squares), compared with pollock length-at-age for winter 2020 (red squares with confidence intervals. Bars indicate  $\pm 1$  standard deviation for the 2020 data.

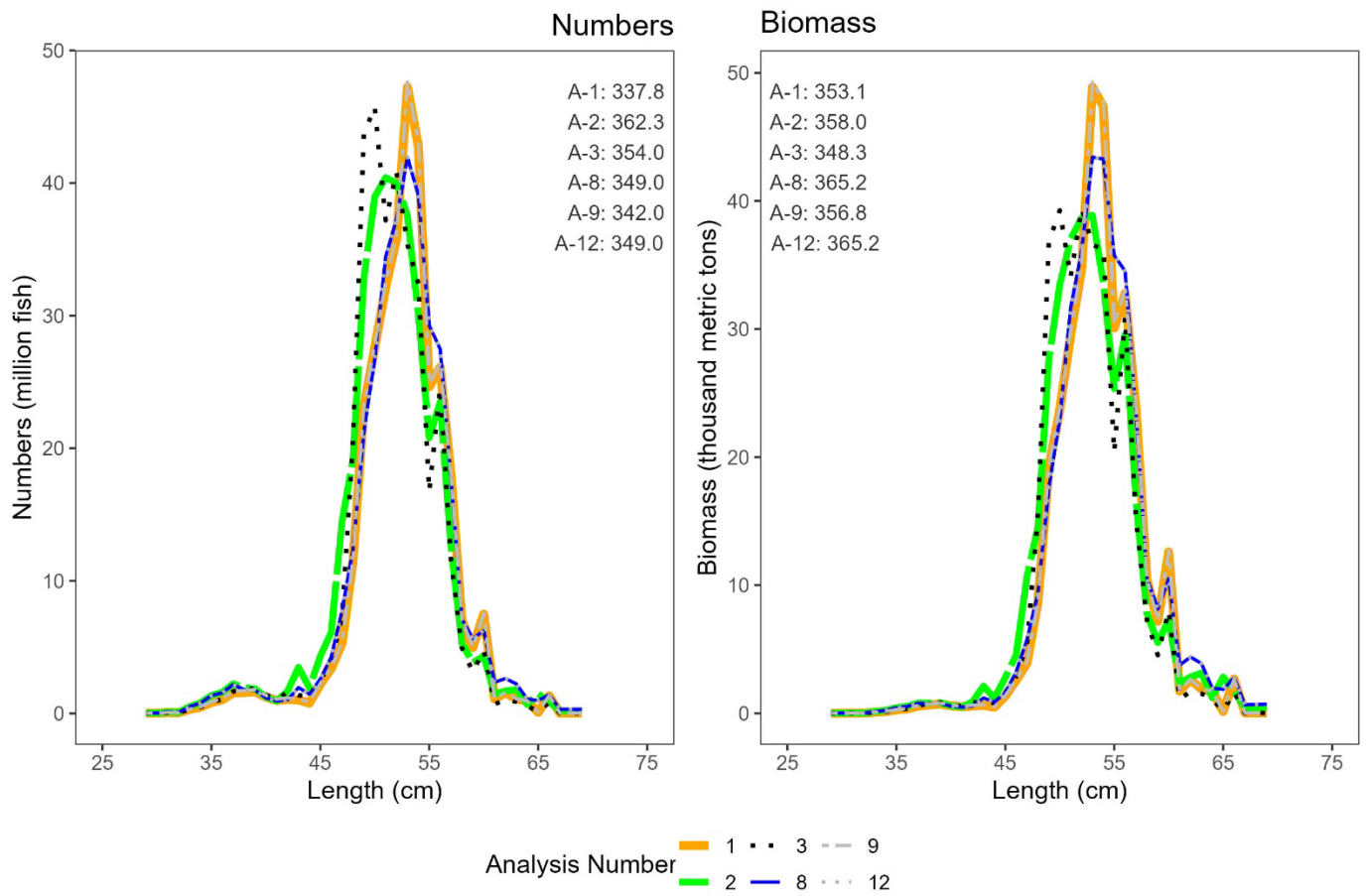


Figure 14. -- Estimated walleye pollock numbers (millions) and biomass (thousand t) at length (cm) comparing results from the 2020 primary analysis (A-1) with results from alternative analyses (A-2, A-3, A-8, A-9, A-12) described in Table 12.



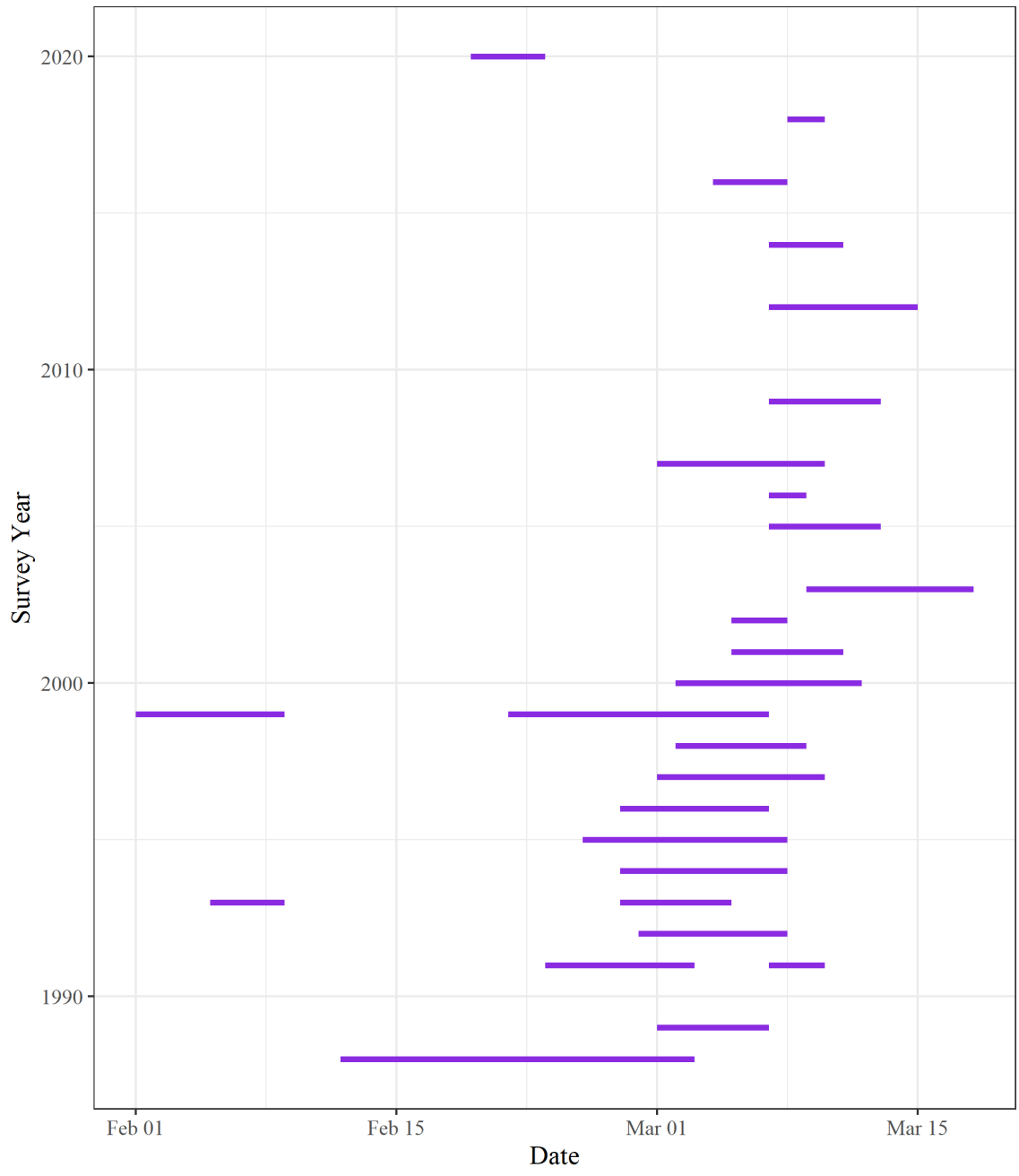


Figure 15. -- Bogoslof acoustic-survey timing conducted by the Alaska Fisheries Science Center and the 1999 survey conducted by Japan.



## Appendix I. Itinerary

### Alaska Standard Time

17 February	Embark scientists in Sand Point, Alaska
18 February	Conduct trawl-sample in Shumagin Islands, Alaska
18 February	Transit towards southeast Aleutian Basin, Alaska
19-23 February	Acoustic-trawl survey of the Bogoslof Island area
24 February	Transit towards Kodiak, Alaska
27 February	Conduct paired-trawls samples in Shelikof Strait, Alaska
28 February	Disembark scientists in Kodiak, Alaska

## Appendix II. Scientific personnel

<u>Name</u>	<u>Position</u>	<u>Organization</u>
Denise McKelvey	Chief Scientist	AFSC
Abigail McCarthy	Fishery Biologist	AFSC
Scott Furnish	Info. Tech. Specialist	AFSC
Heather Kenney	Fishery Biologist	AFSC
Nancy Roberson	Fishery Biologist	AFSC
Mike Levine	Fishery Biologist	AFSC
Ethan Beyer	Fishery Biologist	AIS
Mathew Phillips	Fishery Biologist	AFSC-AIS

AFSC            Alaska Fisheries Science Center, Seattle WA  
AIS             AIS Scientific and Environmental Services, Inc., Marion, MA



### Appendix III. Selectivity correction

Previous research has found that small fish, such as juvenile pollock (fork length < 20 cm) are less likely to be retained by the survey trawl than adults (e.g. Williams et al. 2011). To account for the size and species dependent loss of smaller organisms through the midwater survey trawl meshes ahead of the codend, or “mesh selection”, length compositions were adjusted to that which would be expected from an unselective sampler. Species-specific selectivity relationships describing the probability of retaining a given sized individual were used for the most abundant species, and other species were pooled in broad taxonomic groups. Trawl selectivity  $S_l$  for each cm length class ( $l$ ) of all species or species group caught was estimated by analyzing the catch of the codend and that of small recapture nets mounted on the outside of the trawl during the current survey using methods similar to those presented in Williams et al. (2011). A generalized linear mixed effects model (GLMM) was fitted with a logistic link function and binomial error where variation between tows in selectivity was modeled with random effects.  $S_l$  was then computed as:

$$S_l = \left( 1 + e^{2 \log 3 (LR_{50} - l) / SR} \right)^{-1}, \quad (\text{Eq. i})$$

where  $LR_{50}$  is the length at which 50% of individuals were retained and  $SR$  = selection range (i.e., range in length between 25% and 75% retention values).

These trawl selectivity estimates were then applied to the pollock codend catch composition to correct the sample for escapement from the trawl as:

$$N_{pk\_corr,l} = \frac{N_{pk}}{S_l}, \quad (\text{Eq. ii})$$

where  $N_{sp\_corr,l}$  is the number of fish within a species that would be captured in an unselective sampler in the sampled population and  $N_{sp,l}$  is the number of fish within that species in the 1 cm length class  $l$  in the trawl catch. In analyses with a selectivity correction applied,  $N_{sp\_corr,l}$  was used in place of  $N_{s,l}$  in the abundance calculations (see Appendix IV, Eq. iv).

Selectivity curve estimates and their uncertainty are presented in Table A1 and Figure A1. For the GLMM some hauls with strong outlier estimates of selectivity were further excluded. For all curves, a minimum retention of 0.25% was enforced to prevent overlarge extrapolation errors with model values approaching 0%.

Table A1. -- Selectivity curve estimates for length at 50% retention (*LR50*) and selection range (*SR*) from either the generalized linear mixed effects model (GLMM) or the cumulative GLM for species and groups of species captured in the codend and recapture nets during the winter 2020 acoustic-trawl survey of walleye pollock in the Bogoslof region.

Selectivity group	Model	Length at 50% retention ( <i>LR50</i> )	<i>LR50</i> 95% resample range*	Selection Range ( <i>SR</i> )	<i>SR</i> 95% resample range*	Length range in haul and recapture nets
Age 1+ Pollock LFS	GLMM	9.14	4.31 – 17.00	8.14	4.48 – 12.50	34.7 – 69.3
Age 1+ Pollock AWT	GLMM	11.39	5.50 – 15.11	3.23	5.75 – 12.47	29.1 – 64.3
Generic Fish	GLMM	11.51	9.62 – 15.28	3.79	2.48 – 7.35	2.2 – 69.6
Myctophid	GLMM	7.26	6.48 – 10.12	1.16	0.54 – 5.63	3.5 – 11.7
Non-krill Crustaceans	GLMM	8.32	-3.04 – 24.51	1.7	-7.52 – 14.73	2.5 – 8.9
Squid	Cum. GLM	6.69	5.48 – 9.36	2.26	1.63 – 3.32	1.6 – 16.1

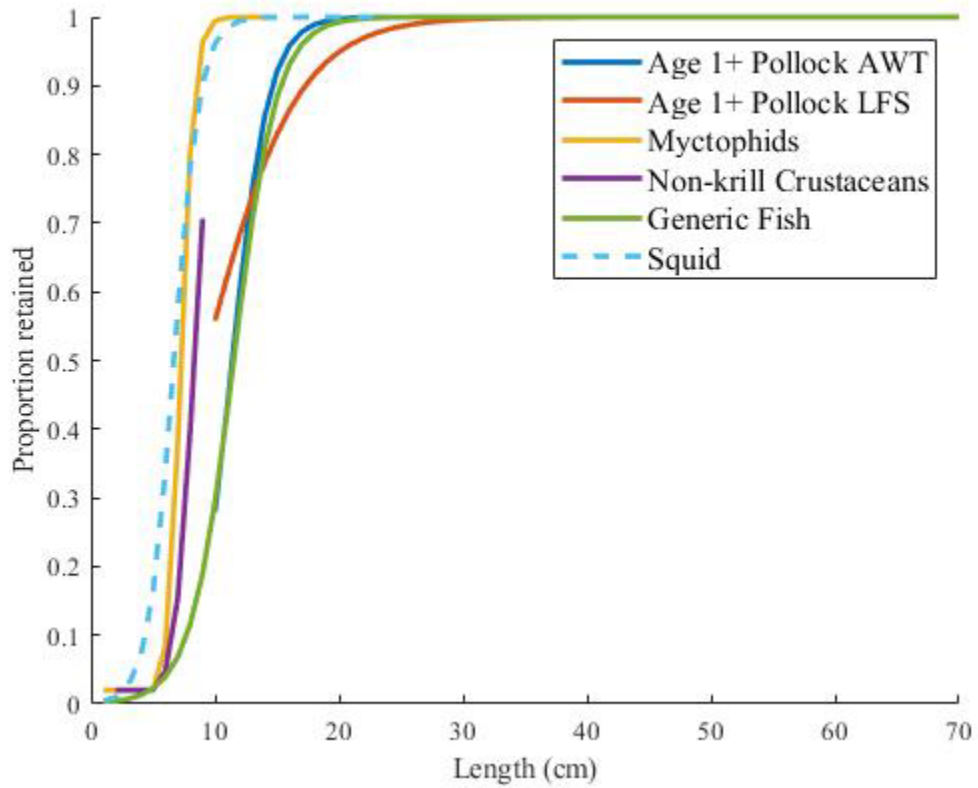


Figure A1. -- Selectivity functions estimated for the DY2002 survey using recapture nets. Selection function values are only plotted for length ranges encountered for each selectivity group.





#### Appendix IV. Abundance calculations

The abundance of target species was calculated by combining the echosounder measurements with size and species distributions from trawl catches and target strength (TS) to length relationships from the literature (see De Robertis et al. 2017 for details). The echosounder measures volume backscattering strength, which is integrated vertically to produce the nautical area scattering coefficient,  $s_A$  (units of  $m^2 \text{ nmi}^{-2}$ ; MacLennan et al. 2002). The backscatter from an individual fish of species  $s$  and at length  $l$  is referred to as its backscattering cross-section,  $\sigma_{bs,s,l}$  ( $m^2$ ), or in logarithmic terms as its target strength,  $TS_{s,l}$  (dB re  $1 m^2$ ), where:

$$TS_{s,l} = 10 \log_{10} (\sigma_{bs,s,l}) \quad . \quad (\text{Eq. iii})$$

The numbers of individuals of species  $s$  in length class  $l$  ( $N_{s,l}$ ) captured in the nearest haul  $h$  were used to compute the proportion of acoustic backscatter associated with each species and length. First, the number of individuals in the catch were converted to a proportion ( $P_{s,l,h}$ ):

$$P_{s,l,h} = \frac{N_{s,l,h}}{\sum_{s,l,h} N_{s,l,h}} \quad , \quad \text{where } \sum_{s,l,h} P_{s,l,h} = 1 \quad . \quad (\text{Eq. iv})$$

In analyses where trawl selectivity was considered, the selectivity-corrected numbers  $N_{s,corr,l,h}$  were used in place of  $N_{s,l,h}$  in Eq. ii. This correction corrects the catch for trawl escapement. The corrected catch is that expected for an unselective sampling device. Refer to the main text for a description of the selectivity corrections applied.

The mean backscattering cross section (an areal measure of acoustic scattering in  $m^2$  – MacLennan et al. 2002) of species  $s$  of length class  $l$  is:

$$\sigma_{bs,s,l} = 10^{(0.1 \cdot TS_{s,l})} \quad , \quad (\text{Eq. v})$$

where TS is the target strength (dB re  $m^2$ ) of species  $s$  at size  $l$ .

The proportion of backscatter from species  $s$  of length class  $l$  in haul  $h$  ( $PB_{s,l,h}$ ) is computed from the proportion of individuals of species  $s$  and length class  $l$  estimated from haul  $h$  ( $P_{s,l,h}$ ) and their backscattering cross section:

$$PB_{s,l,h} = \frac{P_{s,l,h} \cdot \sigma_{bs_{s,l}}}{\sum_{s,l,h} (P_{s,l,h} \cdot \sigma_{bs_{s,l}})} \quad . \quad (\text{Eq. vi})$$

The measured nautical area backscattering coefficient ( $s_A$ ) at interval  $i$  was allocated to species  $s$  and length  $l$  as follows:

$$s_{A_{s,l,i}} = s_{A_i} \cdot PB_{s,l,h} \quad , \quad (\text{Eq. vii})$$

where haul  $h$  is the nearest haul within a stratum assigned to represent the species composition in a given 0.5 nmi along-track interval  $i$ . The nearest geographic haul was determined by using great-circle distance to find the nearest trawl location (defined as the location where the net is at depth and begins to catch fish) out of the pool of hauls assigned to the same stratum (see above for details) closest to the start of interval  $i$ .

The abundance of species of length  $l$  in an area encompassing a series of transect-intervals  $i$  was estimated from the area represented by that interval ( $A_i$ , nmi<sup>2</sup>), the mean areal backscatter attributed to species  $s$  in given length/size class  $l$  ( $s_{A_{s,l,i}}$ , m<sup>2</sup> nmi<sup>-2</sup>), and mean backscattering cross-section of species  $s$  at that size ( $\sigma_{bs_{s,l}}$  m<sup>2</sup>) as follows:

$$\text{Numbers at length } l: N_{s,l} = \sum_i \left( \frac{s_{A_{s,l,i}}}{4\pi\sigma_{bs_{s,l,i}}} \cdot A_i \right) \quad (\text{Eq. viii})$$

$$\text{Biomass at length } l: B_{s,l} = \sum_i (W_{s,l} \times N_{s,l,i}) \quad , \quad (\text{Eq. ix})$$

where  $W_{s,l}$  is the mean weight-at-length for species  $s$  in each 1 cm length  $l$  derived from length-weight regressions. In the case of pollock, when five or more individuals were measured within a length interval, the mean weight at length was used. Otherwise (i.e. for length classes of pollock with <5 weight measurements, or other species), weight-at-length was estimated using a linear regression of the natural log-transformed length-weight data (De Robertis and Williams 2008).

The abundance at age was computed from  $Q_{s,l,j}$ , the proportion of  $j$ -aged individuals of species  $s$  in length class  $l$ , and the abundance of that species and age class in each surveyed interval follows:

$$\text{Numbers at age } j: N_{s,j} = \sum_l (Q_{s,l,j} \times N_{s,l}) \quad (\text{Eq. x})$$

$$\text{Biomass at age } j: B_{s,j} = \sum_l (Q_{s,l,j} \times B_{s,l}) \quad (\text{Eq. xi})$$



U.S. Secretary of Commerce  
**Gina M. Raimondo**

Under Secretary of Commerce for  
Oceans and Atmosphere  
**Dr. Richard W. Spinrad**

Assistant Administrator,  
National Marine Fisheries Service.  
**Janet Coit**

September 2023

[www.fisheries.noaa.gov](http://www.fisheries.noaa.gov)

OFFICIAL BUSINESS

**National Marine  
Fisheries Service**  
Alaska Fisheries Science Center  
7600 Sand Point Way N.E.  
Seattle, WA 98115-6349